AD_____

AWARD NUMBER: W81XWH-09-1-0343

TITLE: Targeting the Kinase-Independent Pro-survival Function of EGFR in Prostate Cancer

PRINCIPAL INVESTIGATOR: Weihua Zhang

RECIPIENT: University of Houston
HOUSTON, TX 77204

REPORT DATE: June 2013

TYPE OF REPORT: Revised Final

PREPARED FOR: U.S. Army Medical Research and Materiel Command
Fort Detrick, Maryland 21702-5012

DISTRIBUTION STATEMENT: Approved for Public Release; Distribution Unlimited

REPORT DOCUMENTATION PAGE	Form Approved OMB No. 0704-0188

1. REPORT DATE (June 2013)	2. REPORT TYPE Revised Final	3. DATES COVERED (04 May 2009 – 03 May 2013)

4. TITLE AND SUBTITLE Targeting the Kinase-Independent, Pro-survival Function of EGFR in Prostate Cancer	5a. CONTRACT NUMBER 5b. GRANT NUMBER W81XWH-09-1-0343 5c. PROGRAM ELEMENT NUMBER
6. AUTHOR(S) Weihua Zhang	5d. PROJECT NUMBER 5e. TASK NUMBER 5f. WORK UNIT NUMBER

7. PERFORMING ORGANIZATION NAME(S) AND ADDRESS(ES) University of Houston, HOUSTON, TX 77204	8. PERFORMING ORGANIZATION REPORT NUMBER
9. SPONSORING/MONITORING AGENCY NAME(S) AND ADDRESS(ES) U.S. Army Medical Research and Materiel Command Fort Detrick, Maryland 21702-5012	10. SPONSOR/MONITOR'S ACRONYM(S) 11. SPONSOR/MONITOR'S REPORT NUMBER(S)

12. DISTRIBUTION/AVAILABILITY STATEMENT
Approved for Public Release; Distribution Unlimited

13. SUPPLEMENTARY NOTES

14. ABSTRACT

The proposed study, targeting the kinase independent pro-survival function of EGFR in prostate cancer, is to investigate the molecular mechanism of EGFR-SGLT1 interaction and test the possibility of use interfering peptides to disrupt the EGFR-SGLT1 interaction for therapeutic purpose, and in parallel to profile the expression status of EGFR/SGLT1 in prostate cancer tissues. Outcomes from this study may lead to find novel strategies for EGFR targeted therapy for prostate cancer.

To date, we have successfully constructed expression plasmids for 12 type of truncated EGFR, which are the key tools to map the interaction domains between EGFR and SGLT1, and we have successfully developed/characterized a polycolonal antibody against human SGLT1 for immunihistochemical staining of human prosate tissues.

15. SUBJECT TERMS none provided

16. SECURITY CLASSIFICATION OF:			17. LIMITATION OF ABSTRACT	18. NUMBER OF PAGES	19a. NAME OF RESPONSIBLE PERSON
a. REPORT	b. ABSTRACT	c. THIS PAGE			19b. TELEPHONE NUMBER (Include area code)

Table of Contents

1. INTRODUCTION:

The epidermal growth factor receptor (EGFR), a receptor tyrosine kinase, is over-active in most of tumors of epithelial origin, and is also correlated with poor prognosis. EGFR is elevated in prostate cancer cells along disease progression. However, EGFR tyrosine kinase inhibitors failed to show any beneficial effects for prostate cancer patients, which raises the question --- *is EGFR tyrosine kinaseactivity the only appropriate target?* Previously, we have found that, independent of its kinase activity,EGFR participates in the maintenance of the basal intracellular glucose level of cancer cells by interacting with and stabilizing sodium-glucose cotransporter 1 (SGLT1), thus preventing cancer cells from autophagic death. This finding unveiled a mechanism of a kinase independent pro-survival function of EGFR. This kinase independent pro-survival function of EGFR may have a great impact in enhancing EGFR targeted prostate cancer therapy, which is strongly supported by our recent preliminary studies. The proposed study, targeting the kinase independent pro-survival function of EGFR in prostate cancer, is to investigate the molecular mechanism of EGFR-SGLT1 interaction and test the possibility of use interfering peptides to disrupt the EGFR-SGLT1 interaction for therapeutic purpose, and in parallel to profile the expression status of EGFR/SGLT1 in prostate cancer tissues. Outcomes from this study may lead to find novel strategies for EGFR targeted therapy for prostate cancer.

2. KEYWORDS: EGFR, SGLT1, glucose, prostate cancer

3. OVERALL PROJECT SUMMARY:

Tasks:

1. To map the SGLT1-interacting/stabilizing domains in EGFR.

a. Create vectors expressing C-terminal myc-tagged EGFR with every 20 amino acids (aa) continuous deletion from its N-terminus. The data is shown in Figure 1.

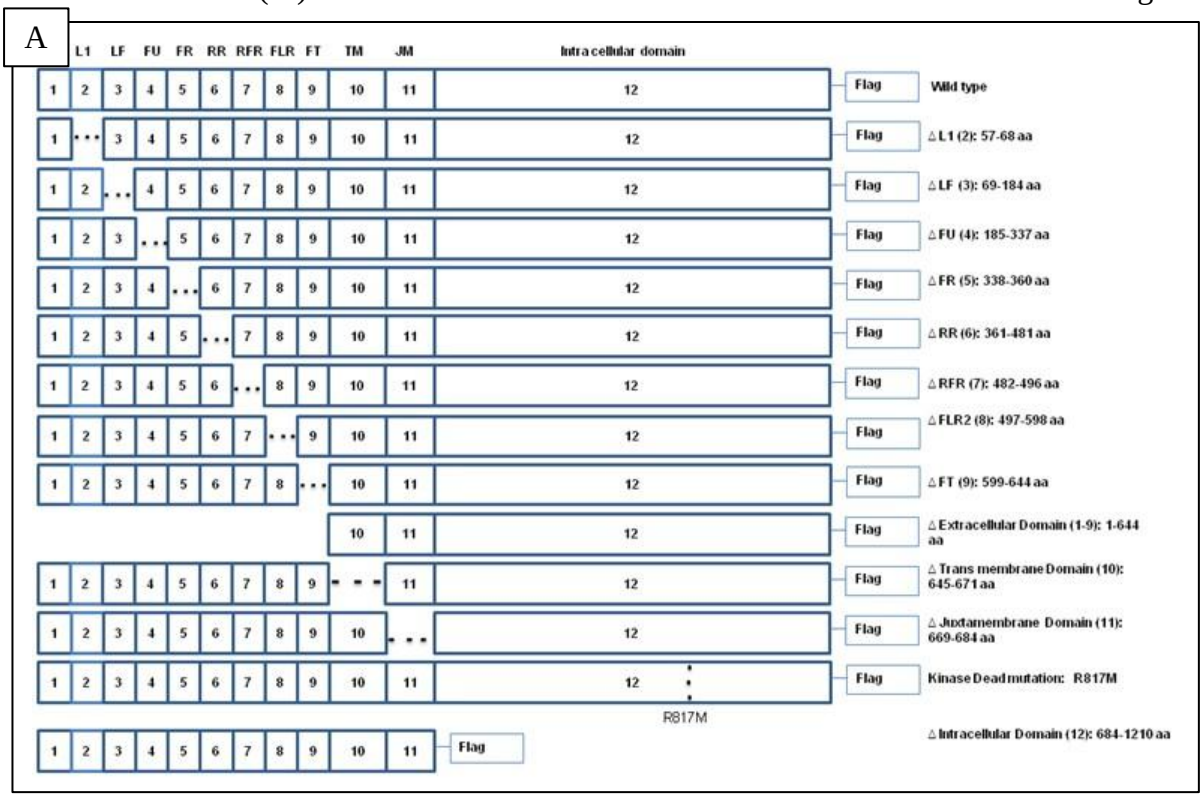

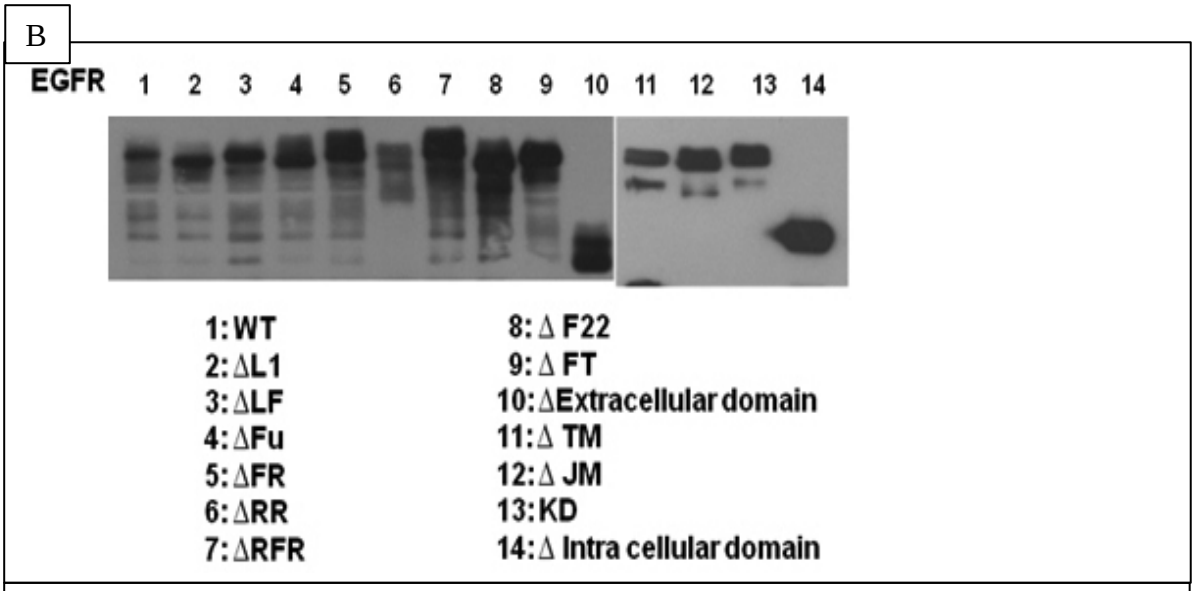

Figure 1. Creation of truncated/mutated EGFR. A, schematic illustration of the mutated region (dash line) in each of EGFR mutant. B, Western Blot analysis of the mutated EGFRs. (these data will be reported in another manuscript that is to be submitted within a month).

b. express these truncated forms of EGFR in either cells harboring endogenous SGLT1 such as prostate cancer PC3MM2 and DU145 cells or these cells overexpressed with exogenous SGLT1 and perform immuno-co-precipitation to determine the interacting domains.

We have found that the major SGLT1 interacting domain of EGFR is its autophosphorylation domain, 978-1120 amino acids. These data are shown in figure 2, and reported in Publication Ref. #1.

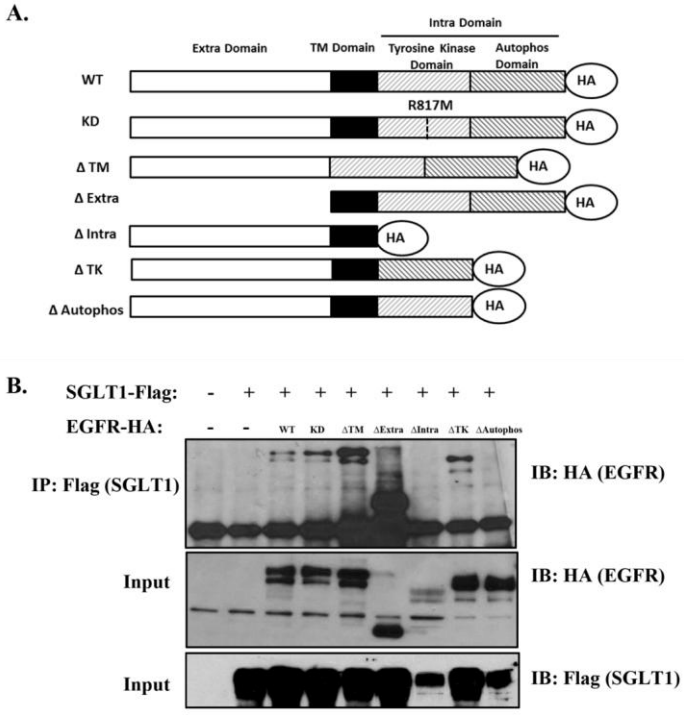

Figure 2. The autophosphorylation domain of EGFR is required for its interaction with SGLT1. A, Schematic diagram of constructs of human EGFR used in this study: WT, wild type EGFR; KD, kinase dead EGFR (R817M); ΔTM, transmembrane domain deletion (645-670aa); ΔExtra, extracellular domain deletion (1-644aa); ΔIntra, intracellular domain deletion (671-1210aa); ΔTK, tyrosine kinase domain deletion (670-977aa); ΔAutophos, autophosphoralization domain deletion (978-1210aa). B, Deletion of the entire intracellular domain or the autophosphorylation domain of EGFR significantly reduced its interaction with SGLT1. C, By increasing the expression level of the ΔIntra-EGFR, the ΔIntra-EGFR was co-precipitated with SGLT1. Immunoprecipitation coupled Western blot analysis of interactions between mutated EGFRs and SGLT1. IP, immunoprecipitation. IB, Immunoblot. Input, expression levels of indicated exogenous proteins in HEK293 whole cell lysates used for the IP. EGFR bands are indicated by arrowheads. Non-specific bands (NS) are indicated by arrows.

c. Co-express full length SGLT1 with truncated forms of EGFR in HEK293 cells and determine the stability of SGLT1 expression in these cells.

We have found that expression of the SGLT1 interacting domain deleted EGFR destabilizes SGLT1 protein, which is shown in figure 3. These data have been reported in Publication Ref. #1.

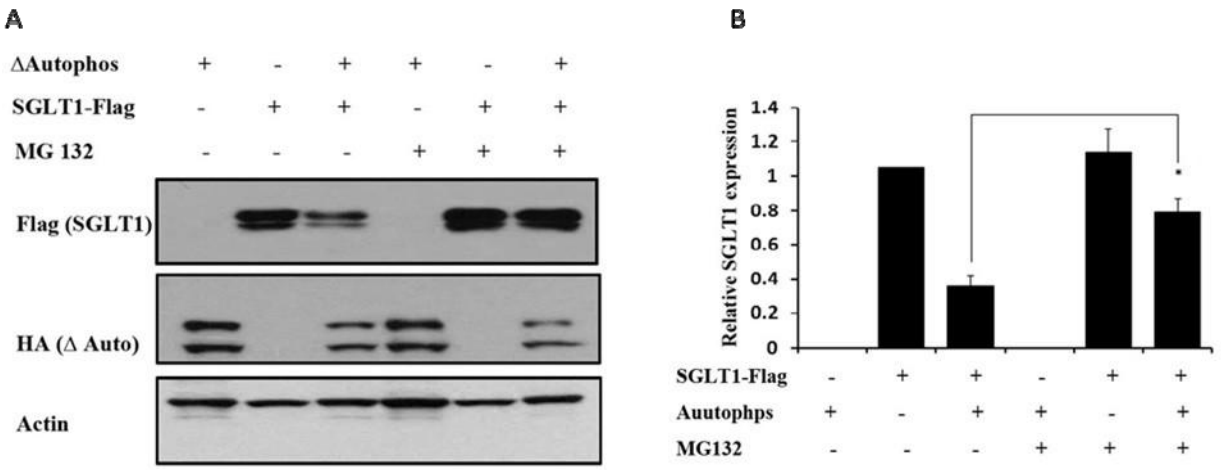

Fig. 2. The autophosphorylation domain of EGFR is required to prevent proteasome mediated SGLT1 degradation. A, Western blot analysis of expression levels of SGTL1 in HEK293 cells co-transfected with the WT-EGFR, the KD-EGFR and the ΔAutophos-EGFR. The same amounts of DNA plasmids of SGLT1 and EGFRs were used in each group of treatments. Control cells were transfected with the same amount DNA of the empty vector. Actin was used as loading control. B, Densitometric quantification of bands in the Western blot of Figure 2A. Asterisk marks indicate statistic significance between the linked representative group from triplicate experiments. C, Proteasome inhibitor MG132 blocked the down-regulation of SGLT1 by ΔAutophos-EGFR. Actin was used as a loading control. D, Densitometric quantification of bands in the Western blot of Figure 2A. Asterisk marks indicate statistic significance between the linked representative group from triplicate experiments.

ACCOMPLISHMENTS

We have successfully accomplished this task. We found that the C-terminal autophosphorylation domain of EGFR is the major SGLT1 interacting domain. We have reported this finding in a manuscript that was accepted for publication two weeks ago (attachment #1)(Ref. 1).

2. To test whether cell survival is compromised upon disruption of the interaction between EGFR and SGLT1 by interfering peptides.

a. design interfering peptides that have the similar sequence as the SGLT1-interacting domains of EGFR.

b. create vectors expressing these interfering peptides identical to the interacting domains and chemically synthesize these peptides.

c. treat prostate cancer cells, PC3-MM2 and DU145, with the interfering peptides, and determine the survivability of the treated cells as compared with control cells.

ACCOMPLISHMENTS

We have tested 7 peptide candidates, and one of the 7 peptides showed effectiveness in down-regulating EGFR and SGLT1, and decreasing the survivability of PC3 cells (data shown below in Figure 3). A provisional patent has been filled. Data will be published in another manuscript after filling a non-provisional patent.

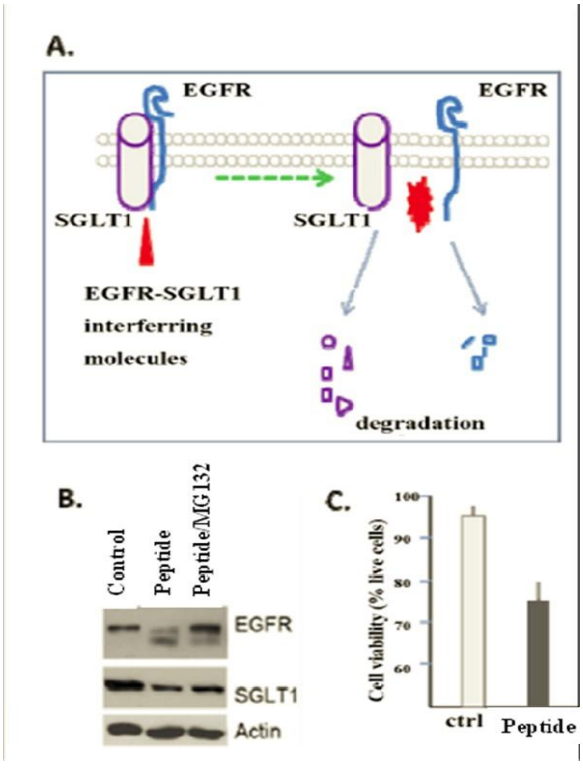

Figure 3. An EGFR-SGLT1 interfering peptide destabilized EGFR and SGLT1 and decreased cell viability of prostate cancer PC3 cells. (A), schematic illustration of the principle of disrupting EGFR-SGLT1 interaction by small molecules. (B), Western Blot analysis of EGFR and SGLT1 levels in cells treated with the interfering peptide with/without a proteasome inhibitor MG132. (C), trypan blue uptake assay on cell viability of PC3 cell treated by ESD-01 for 12hr.

3. To profile the expression of SGLT1 and EGFR in tissues of well characterized prostate cancer tissues.

We have accomplished this task. We found that SGLT1 and EGFR colocalized in all EGFR positive prostate cancer tissues tested (n=41), which are shown in Figure 4 and 5. These data were included in the manuscript (attachment #1, #2) (1, 2).

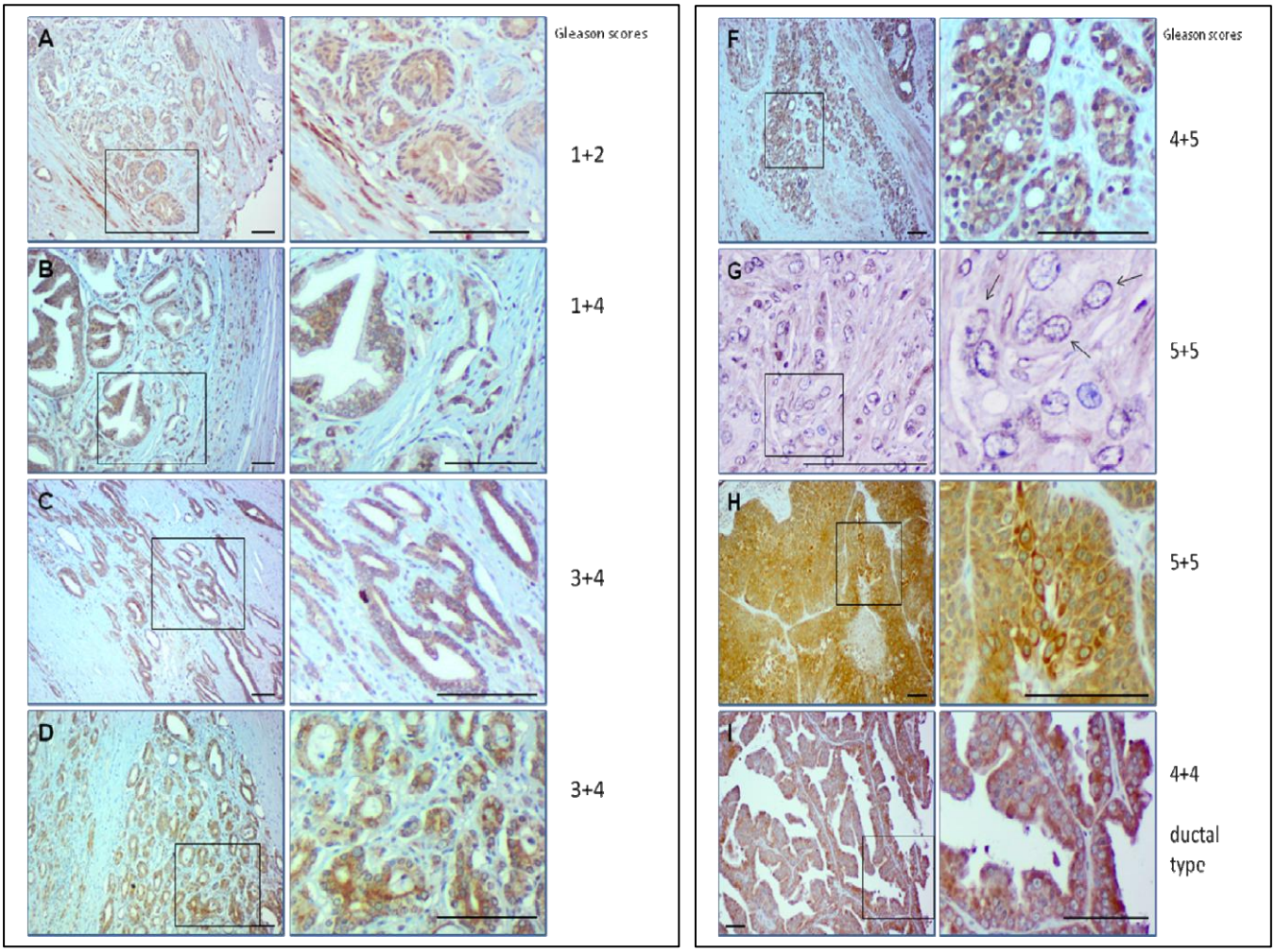

Figure 4.Expression of SGLT1 in PCa tissue representing different grades (Gleason scores). (**A-I**), SGLT1-positive cells appear brown. Arrows in **G** indicate SGLT1-positive nuclear envelopes. Right panels are magnification of boxed areas in left panels. Bar=50µm.

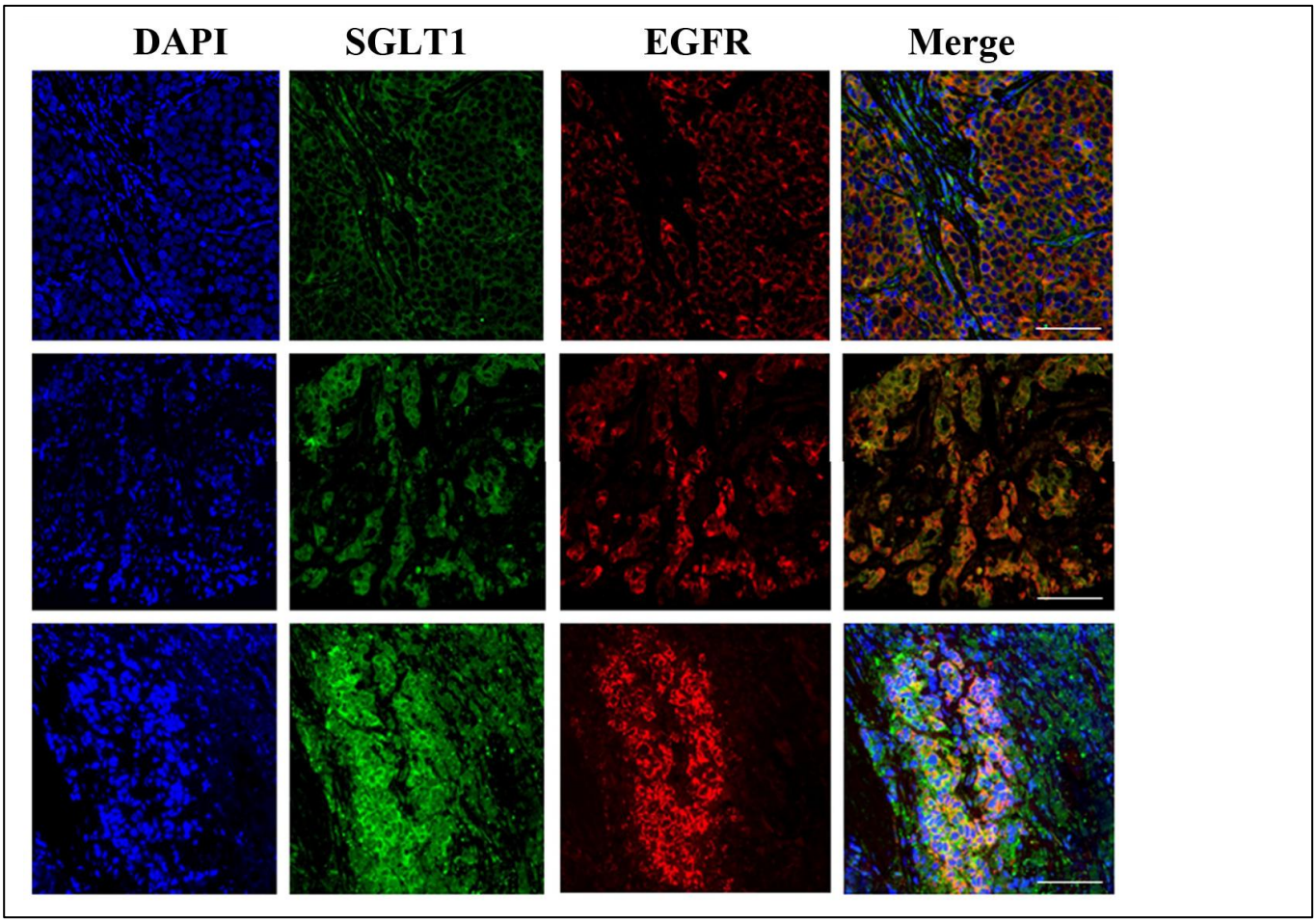

Figure 5. Co-localization of EGFR and SGLT1 in prostate cancer tissues by immunofluorescent co-staining and inhibition of SGLT1 by a SGLT1 inhibitor sensitized prostate cancer cells to EGFR inhibitors. A, Results of three representative prostate cancer tissues from a prostate cancer tissue array are presented. Co-localization of SGLT1 (green) and EGFR (red) are in colors of orange or yellow (arrows). Bar=100 μm.

4. KEY RESEARCH ACCOMPLISHMENTS:

Overall, we have achieved all the research goals.

1. The major SGLT1 interacting domain in EGFR protein has been identified, the autophosphorylation domain of EGFR (Ref. 1).
2. An EGFR-SGLT1 interaction interfering peptide has been synthesized and tested in Vitro (Figure in this report and a filled provisional Patent).
3. We have shown that loss of interaction between EGFR and SGLT1 lead to destabilization of each of the proteins (Ref. 1).
4. We have reported that SGLT1 is over-expressed in prostate cancer tissues and colocalized with EGFR (Ref. 2).
5. We have shown that loss of EGFR protein, but not inhibition of it tyrosine kinase activity, sensitized prostate cancer cells to chemotherapeutic reagents (Ref. 3).
6. We have shown that targeting SGLT1 could sensitize prostate cancer cells to EGFR tyrosine kinase inhibitors (Ref. 1).

5. CONCLUSION:

The tyrosine kinase activity of EGFR has served as the primary target for EGFR based cancer therapies. At the clinic, inhibition of the tyrosine kinase of EGFR by small molecules has produced responding rates ranging between 10-20% across a variety of human malignancies, however, with no exception of development of drug resistance within few months after treatment. Mechanisms whereby cancers primarily resist or acquire resistance to EGFR tyrosine kinase inhibitor (TKi) have been largely attributed to the gain of functions of EGFR and/or other pro-survival signalings subsequent to inhibition of EGFR tyrosine kinase. A critical question remains to be answered is that "*why there are patients bearing EGFR overexpressing cancers do not response to EGFR TKi?"* Prostate cancer (PC) is one representative type cancer wherein EGFR expression increases along with disease progression, but, in general, it is highly resistant to EGFR TKi treatment.

Our study has found that EGFR in cancer cells can exist as either a tyrosine kinase modulator responsive status or an irresponsive status. SGLT1 is a protein involved in EGFR's functions that are irresponsive to EGFR tyrosine kinase inhibitors, EGFR and SGLT1 colocalized in prostate cancer cells, and disruption the EGFR-SGLT1 interaction decreased the survivability of prostate cancer cells and, targeting EGFR-SGLT1 interaction shall be a novel therapeutic approach for prostate cancer treatment.

6. PUBLICATIONS, ABSTRACTS, AND PRESENTATIONS:

a. Publications

(1) Lay Press: None

(2) Peer-Reviewed Scientific Journals:

1. Xu S. and Weihua Z. Loss of EGFR induced autophagy sensitizes hormone refractory prostate cancer cells to adriamycin. Prostate, 17:1216-1224, Aug., 2011. doi: 10.1002/pros.21337
2. Bollu RL, Ren J, Chen J, Gao G and Weihua Z. Epidermal Growth Factor Receptor in Prostate Cancer Cells (Book Chapter), in Detection, Growth and Treatment of Prostate Cancer. Nova Publishers, 147-160, 2012.
3. Blessing A, Xu L, Gao G, Bollu LR, Ren J, Li H, Wu X, Su F, Huang W-C, Hung M-C, Huo L, Palapattu GS and Weihua Z. Sodium/Glucose Co-transporter 1 Expression Increases in Human Diseased Prostate. J Cancer Sci. Ther., 4: 306-312, 2012. doi:10.4172/1948-5956.1000159

(3) Manuscripts

1. Bollu RL, Ren J, Gao G, Xu L, Wang J, Su F and Weihua Z. De novo synthesized palmitate mediates the activation of mitochondrial EGFR by plasma membranous EGFR to promote mitochondrial fusion in cancer cells. 2013 (submitted).
2. Ren J, Wang J, Brasher H, Xu L, Bollu RL, Chen J, Gao G, Su F, Palapattu G, Widger WR and Weihua Z. Mitochondrial EGFR induces aerobic glycolysis of cancer cells independent of its kinase activity. 2013 (manuscript to be resubmitted in two months).

(4) Invited Articles:

Bollu RL, Ren J, Chen J, Gao G and Weihua Z. Epidermal Growth Factor Receptor in Prostate Cancer Cells (Book Chapter), in Prostate Cancer Cells: detection, growth and treatment . Nova Publishers, 147-160, 2012.
https://www.novapublishers.com/catalog/product_info.php?products_id=39458

(5) Abstracts:

Title: Profiling the expression of SGLT1 in prostate cancer
Authors; Alicia Blessing, Zhang Weihua
Meeting: AACR 102nd Annual Meeting 2011-- Apr 2-6, 2011; Orlando, FL
DOI: 10.1158/1538-7445.AM2011-989

7. INVENTIONS, PATENTS AND LICENSES:

Inventor: Zhang Weihua
Invention title: **Targeting EGFR-SGLT1 interaction for cancer therapy**
Patent application number: UHID-2013-014(Provisional)
Filing date: 05-03-2013

8. REPORTABLE OUTCOMES:

1. Antibodies against SGLT1 for Immunohistochemical staining and Western Blot analysis respectively.
2. An EGFR-SGLT1 interaction interfering peptide has been synthesized.
3. We have found that SGLT1 is over expressed in Prostate Cancer Tissues.
4. We have found that SGLT1 is over-expressed in Benign Prostatic Hyperplasia
5. We have found that SGLT1 is co-localized with EGFR in Prostate Cancer Tissues.
6. We also found that loss of EGFR protein but not inhibiting its tyrosine kinase activity was effective in sensitizing prostate cancer cells to chemotherapeutic reagents (Ref. 3).
6. We have identified that the major SGLT1 interacting domain in EGFR is its autophosphorylation domain.
7. Our data suggest that there are EGFRs that will never be activated by phosphorylation, yet play critical pro-survival roles in prostate cancer, which is a significant conceptual advancement in our understanding EGFR functions in prostate cancer.

9. OTHER ACHIEVEMENTS:

1. An NIH-RO1 proposal entitled : Novel Functions of EGFR in Prostate Cancer Resistance to EGFR Tyrosine Kinase Inhibition, has been Submitted on June 5, 2013.
2. An NIH-R21 proposal entitled: Per1 regulated SGLT1 expression in the pathogenesis of BPH during ageing**,** was submitted Oct. 16, 2012, and will be re-submitted June 16, 2013.
3. Graduate Students Jinyu Chen, Lakshmi Bollu, and Alicia Blessing, have been partially supported by this grant. They all will be graduating within a year.

10. REFERENCES:

1. Ren J, Bollu LR, Su F, Gao G, Xu L, Huang W-C, Hung M-C and Weihua Z. EGFR-SGLT1 interaction does not respond to EGFR modulators, but inhibition of SGLT1 sensitizes prostate cancer cells to EGFR tyrosine kinase inhibitors. Prostate, 2013 (in press, attached).
2. Blessing A, Xu L, Gao G, Bollu LR, Ren J, Li H, Wu X, Su F, Huang W-C, Hung M-C,

Huo L, Palapattu GS and Weihua Z. Sodium/Glucose Co-transporter 1 Expression Increases in Human Diseased Prostate. J Cancer Sci. Ther., 4: 306-312, 2012. doi:10.4172/1948-5956.1000159

3. Xu S. and Weihua Z. Loss of EGFR induced autophagy sensitizes hormone refractory prostate cancer cells to adriamycin. Prostate, 17:1216-1224, Aug., 2011. doi: 10.1002/pros.21337

11. APPENDICES:

Original copy of three articles and one abstract.

Journal	MSP No.	Dispatch: May 25, 2013	CE: Vaishnavi
PROS	22692	No. of Pages: 9	PE: Alyson Linefsky

The Prostate 9999:1^9 (2013)

EGFR^SGLT1 Interaction Does Not Respond to EGFR Modulators, But Inhibition of SGLT1 Sensitizes Prostate Cancer Cells to EGFR Tyrosine Kinase Inhibitors

Jiangong Ren,[1] Lakshmi R. Bollu,[1] Fei Su,[1] Guang Gao,[1] Lei Xu,[1] Wei-Chien Huan [2] Mien-Chie Hung,[2,3] and Zhang Weihua[1]*

[1]Department of Biology and Biochemistry, College of Natural Sciences and Mathematics, University of Houston, Houston, Texas

[2]Center for Molecular Medicine, China Medical University Hospital, Taichung, Taiwan

[3]Department of Molecular and Cellular Oncology, The University of Texas MD Anderson Cancer Center, Houston, Texas

BACKGROUND. Overexpression of epidermal growth factor receptor (EGFR) is associated with poor prognosis in malignant tumors. Sodium/glucose co-transporter 1 (SGLT1) is an active glucose transporter that is overexpressed in many cancers including prostate cancer. Previously, we found that EGFR interacts with and stabilizes SGLT1 in cancer cells.

METHODS. In this study, we determined the micro-domain of EGFR that is required for its interaction with SGLT1 and the effects of activation/inactivation of EGFR on EGFR–SGLT1 interaction, measured the expression of EGFR and SGLT1 in prostate cancer tissues, and tested the effect of inhibition of SGLT1 on the sensitivity of prostate cancer cells to EGFR tyrosine inhibitors.

RESULTS. We found that the autophosphorylation region (978–1210 amino acids) of EGFR was required for its sufficient interaction with SGLT1 and that this interaction was independent of EGFR's tyrosine kinase activity. Most importantly, the EGFR–SGLT1 interaction does not respond to EGFR tyrosine kinase modulators (EGF and tyrosine kinase inhibitors). EGFR and SGLT1 co-localized in prostate cancer tissues, and inhibition of SGLT1 by a SGLT1 inhibitor (Phlorizin) sensitized prostate cancer cells to EGFR inhibitors (Gefitnib and Erlotinib).

CONCLUSION. These data suggest that EGFR in cancer cells can exist as either a tyrosine kinase modulator responsive status or an irresponsive status. SGLT1 is a protein involved in EGFR's functions that are irresponsive to EGFR tyrosine kinase inhibitors and, therefore, the EGFR–SGLT1 interaction might be a novel target for prostate cancer therapy. Prostate 9999:1–9, 2013. Published 2013 Wiley Periodicals, Inc.[y]

KEY WORDS: EGFR; SGLT1; glucose; cancer; prostate

INTRODUCTION

Epidermal growth factor receptor (EGFR) is a receptor tyrosine kinase that is over-active/over-expressed in the majority cancers of epithelial origin [1]. Inhibition of the tyrosine kinase activity of EGFR has been the principle strategy of EGFR based cancer therapies. However, targeting EGFR by small molecule inhibitors of receptor tyrosine kinase has produced disappointing response rates ranging between 10% and 20% across a variety of human

Grant sponsor: American Cancer Society; Grant number: RSG-09-206-01; Grant sponsor: Department of Defense Prostate Cancer Research Program; Grant number: W91ZSQ8334N607; Grant sponsor: University of Houston.

The authors declared that they have no conflicts of interest.

*Correspondence to: Zhang Weihua, Department of Biology and Biochemistry, College of Natural Sciences and Mathematics, University of Houston, Houston, TX 77204-5001.
E-mail: wzhang13@uh.edu

Received 5 March 2013; Accepted 2 May 2013
DOI 10.1002/pros.22692
Published online in Wiley Online Library (wileyonlinelibrary.com).

malignancies [2–4]. For example, although EGFR is overexpressed in more than 80% of late stage prostate cancers and is negatively correlated with prognosis [5–8], in general, prostate cancer is resistant to EGFR inhibitors [9,10].

Evidence indicates that EGFR has tyrosine kinase independent functions. While EGFR knockout animals die soon after birth [11], mice with severely compromised EGFR tyrosine kinase activity are viable and display only some epithelial defects [12]. Both a wild-type and a kinase-dead EGFR enhance the survival of EGFR-negative 32D hematopoietic cells [13]. Previously, we found that, independent of EGFR tyrosine kinase activity, EGFR participates in the maintenance of basal intracellular glucose level of cancer cells by interacting with and stabilizing the sodium/glucose co-transporter 1 (SGLT1) [14].

SGLT1 is an active glucose transporter that relies on extracellular sodium concentration to transport glucose into cells independent of glucose concentration [15]. SGLT1 plays a critical role in glucose absorption and retention in the body [16]. One of the hallmarks of cancer is that cancer cells exhibit altered energy metabolism, that is, cancer cells consume higher amounts of nutrients and energy substrates than their normal counterparts [17]. This enhanced energy consumption demands a high rate of nutrient uptake, which is achieved by overexpression of plasma membrane transporters [18]. SGLT1 is overexpressed in various types of cancers including ovarian carcinoma [19], oral squamous cell carcinoma [20], colorectal cancer [21], pancreatic cancer [22], and prostate cancer [23]. Prostate cancers at late stages express elevated levels of EGFR [5–7] and uptake a high amount of glucose [24,25]. Whether the relationship between EGFR and SGLT1 can be manipulated for therapy of prostate cancer remains unknown.

In this study, we characterized the critical domain of EGFR that is required for its sufficient interaction with SGLT1. We also determined the effects of activation/inactivation of EGFR tyrosine kinase activity on EGFR–SGLT1 interaction, measured the expression of EGFR and SGLT1 in prostate cancer tissues, and tested the effect of inhibiting SGLT1 on the sensitivity of prostate cancer cells to EGFR inhibitors.

MATERIALS AND METHODS

Cells and Reagents

HEK293 cell lines, prostate cancer cell line PC3 and LNCaP, were originally purchased from the American Type of Culture Collection (ATCC) and maintained in DMEM supplemented with 10% fetal bovine serum and 1% penicillin/streptomycin under 5% CO_2 at 37°C. Mouse anti-Flag-tag antibody (F1804), proteasome inhibitor MG132, and Phlorizin dihydrate were from Sigma-Aldrich (St. Louis, MO). AEE788, Gefitinib, and Erlotinib were purchased from Selleckchem (Houston, TX). Antibody against pEGFR (Y1173) (cat. no. 2434L) was from Cell Signaling (Danvers, MA). Monoclonal antibody against C225 was a gift from Dr. Lee Elis (M. D. Anderson Cancer Center, Houston, TX). Rabbit anti-actin (cat. no. sc-7210), rabbit anti-HA-tag antibody (sc-805), secondary antibodies against rabbit and mouse labeled with horseradish peroxidase, and protein A/G conjugated agarose beads (cat. no. sc-2003) were from Santa Cruz Biotechnology (Santa Cruz, CA). MTT kit (cat. no.30-1010K) was from ATCC. The plasmid expressing flag tagged human SGLT1 and the rabbit anti-human-SGLT1 polyclonal antibodies for immunohistochemical analysis (SGLT1-IHC), immunoprecipitation, and Western blotting analysis (SGLT1-WB) were described previously [23].

Plasmid Constructions

Human wild-type EGFR was cloned into a pcDNA3.1 vector (Clontech, CA), which was used as a parental vector to generate all the other EGFR constructs. The pRK5 expression plasmid (Clontech) with a c-terminal HA tags was used for constructions of all the HA tagged EGFRs. The full-length human EGFR was amplified with a forward primer EGFR-F (ATTCTCGAGCGGGGAGCA GCGATG) and a reverse primer EGFR-R (CCTAAGCTTTGCTCCAA-TAAATTCACTG). DNA fragments were digested by Xho I and Hind III and cloned into the corresponding sites of the pRK5 vector. Primers for cloning the EGFR with extracellular domain deletion (DExtra, 1–644aa) are DExtra-F: ATTCTCGAGATGTCC ATCGCCACTG-GGATG and DExtra-R: CCTAAGCTTTGCTCCAA-TAAATTCACTGC; primers for intracellular deletion (DIntro, 671–1210aa) are DIntra-F: TATCTCGAGATG-CGACCCTCCGGGACGGC and DIntra-R: CCTAAG-CTTCC TTCGCATGAAGAGGCC; primers for autophosphorylation domain deletion (DAutophos, 978–1210aa) are DAutophospho-F: ATTCTCGAGATGTC-CATCGCCACTGGGATG and DAutophospho-R: CC-TAAGCTT GTAGCGCTGGGGGTCTCGG; primers for intracellular domain deletion (645–1210aa) are DIntra-F: TATCTCGAGATGCGACCCTCCGGGACGGC and DIntra-R: CCTAAGCTTCCTTCGCATGAAGAGGC. The kinase dead mutant of EGFR (KD-EGFR, R817M), transmembrane domain deletion (DTM, 645–670aa), tyrosine kinase domain deletion (DTK, 670–977aa) plasmids were constructed from pRK5-WT-EGFR-HA by site-directed mutagenesis using the QuikChange

Lightning Site-Directed Mutagenesis Kit (Agilent, CA) according to the manufacturer's protocol. The primers were: KD-EGFR-F: GCACCGCGACCTGGCAGCC ATGAACGTACTGGTGAAAACACC and KD-EGFR-R: GGTGTTTTCACCAGTACGTTCATGGCTGCCA GGTCGCGGTGC; DTM-F: CGAGACCCCCAGCGCTACCGGACTCCCCTCCTGAGC and DTM-R: CGAGACCCCCAGCGCTACCGGACTCCCCTCCTGAGC; DTK-F: CGCTGCGGAGGCTGCTGCAGTAC CTTGTCATTCAGGGGG and DTK-R: CCCCCTGAATGCAAGGTACTGCAGCAGCCTCCGCAGCG. All of the constructs yielded fusion proteins with a C-terminal HA tag. All plasmids were confirmed by sequencing.

Transient Transfection and Immunoprecipitation

HEK293 cells were transfected with plasmids expressing flagged SGLT1 alone or with indicated HA-tagged EGFR constructs. After 24 hr of transfection, cells were washed in 1× phosphate-buffered solution and lysed with RIPA buffer (50 mM Tris–HCl, pH 8.0, with 150 mM sodium chloride, 1.0% Igepal CA-630 (NP-40), 0.5% sodium deoxycholate, and 0.1% sodium dodecyl sulfate), supplemented with protease inhibitors cock tail, for 6 hr on a shaker at 4°C. The cell lysates were then centrifuged for 2 min at 12,000× rpm. Supernatants were then incubated with sepharose protein A/G beads conjugated with anti-flag or anti-SGLT1 antibody overnight at 4°C. Samples were then centrifuged and washed with RIPA buffer three times before being boiled in Laemmli buffer (Biorad, CA) and subjected to Western blot (WB) analysis. To determine the role of EGFR's tyrosine kinase in EGFR–SGLT1 interaction, HEK293 cells were transfected with SGLT1 with/without wild-type EGFR. After 18 hr, cells were starved in serum-free medium for 6 hr before treatment with EGF (10 ng/ml), or EGF plus AEE788 (5 mM) for 30–60 min. Control cells were treated with an equal volume of vehicle dimethyl sulfoxide (DMSO). Cell lysates were then subjected to immunoprecipitation as described above.

Western Blot Analysis

For WB analysis, cells were lysed with RIPA buffer (150 mM NaCl, 50 mM Tris–HCl, pH 7.4, 0.1% SDS, 1% Triton X-100, 1 mM EDTA, 1 mM PMSF, 20 mg/ml aprotinin, 20 mg/ml leupeptin, 20 mg/ml pepstatine, 1% sodium deoxycholate, 1 mM NaF, 1 mM Na_3VO_4, in H_2O). Proteins separated by 8% SDS–PAGE were transferred to PVDF membrane followed by blocking with 5% nonfat dry milk and then incubation with primary antibodies at optimized concentrations for overnight at 4°C. The membranes were washed with 0.1% TBS/T (1× TBS, 0.1% Tween-20) three times, each time for 5 min before incubation with secondary antibody for 1 hr at room temperature and signals were visualized by enhanced chemiluminescence.

Immunofluorescent Co-Staining

For immunofluorescent co-staining of SGLT1 and EGFR, slides of prostate cancer tissue array were deparrafinated, rehydrated before antigens were retrieved in boiling citrate buffer for 10 min. Cooled tissue slides were then incubated in a blocking solution (5% donkey serum in PBS) for 1 hr at room temperature and then overnight at 4°C with the rabbit polyclonal antibody against SGLT1 (SGLT1-IHC) [23] (1:200 dilution) and C225 1:200 in PBS containing 10% donkey serum. After being washed three times with PBS, tissues were incubated with a mixture of Alexa Fluor 488-conjugated donkey anti-rabbit IgG and Alexa Flour 594-conjugated donkey anti-mouse IgG dissolved in PBS containing 10% donkey serum for 30 min at room temperature. The stained samples were then washed three times (5 min per wash) with PBS at room temperature. Fluorescence images were captured and analyzed with a confocal microscope (Olympus). Cell nucleus was stained by 4′,6-diamidino-2-phenylindole (DAPI).

Cell Growth Assay

Cell growth was determined by 3-(4,5-dimethylthiazole-2-yl)-2,5-diphenyltetrazolium bromide (MTT) assay in 96-well plates according to the protocol provided by the manufacture. Briefly, 5,000 cells suspended in 100 ml medium were seeded in each well of a 96-well plate. On the second day, medium was replaced by medium containing Phlorizidin[Q2] (50 mM) with/without EGFR inhibitors (Gefitinib: 20 mM; Erlotinib: 20 mM). After 24 or 48 hr incubation with drugs, 10 ml MTT reagents was added to each well and incubated for 4 hr. After removal of the medium, the formazan precipitates in cells were dissolved in 100 ml DMSO. Absorbance was measured by a MultiSkan plate reader (Thermo Fisher Scientific, NC) at 570 nm. Triplicates of samples in each group were used.

Statistical Analysis

The Student's t-test was used to assess the difference in growth of cells treated with EGFR inhibitors in the presence/absence of SGLT1 inhibitor. P values less than 0.05 were defined as statistical significance.

RESULTS

The Autophosphorylation Domain of EGFR Is Critical for Its Sufficient Interaction With SGLT1, Which Is Independent of EGFR Tyrosine Kinase Activity

Previously, we reported that the extracellular domain containing the transmembrane domain of EGFR interacted with SGLT1 and the intracellular domain without the transmembrane domain did not sufficiently interact with SGLT1 [14]. To further determine the region in EGFR protein that is critically required for its interaction with SGLT1, we created flag-tagged SGLT1 [23] and HA-tagged EGFRs with a variety of mutations. These mutated EGFRs include a kinase dead form (R817M) (KD-EGFR), an extracellular domain deleted form (DExtra), a transmembrane domain deleted form (DTM), an intracellular domain deleted form (DIntra), a tyrosine kinase domain deleted form (DTK), and an autophosphorylation domain deleted form (DAutoPhos) (Fig. 1A). We transiently co-transfected an

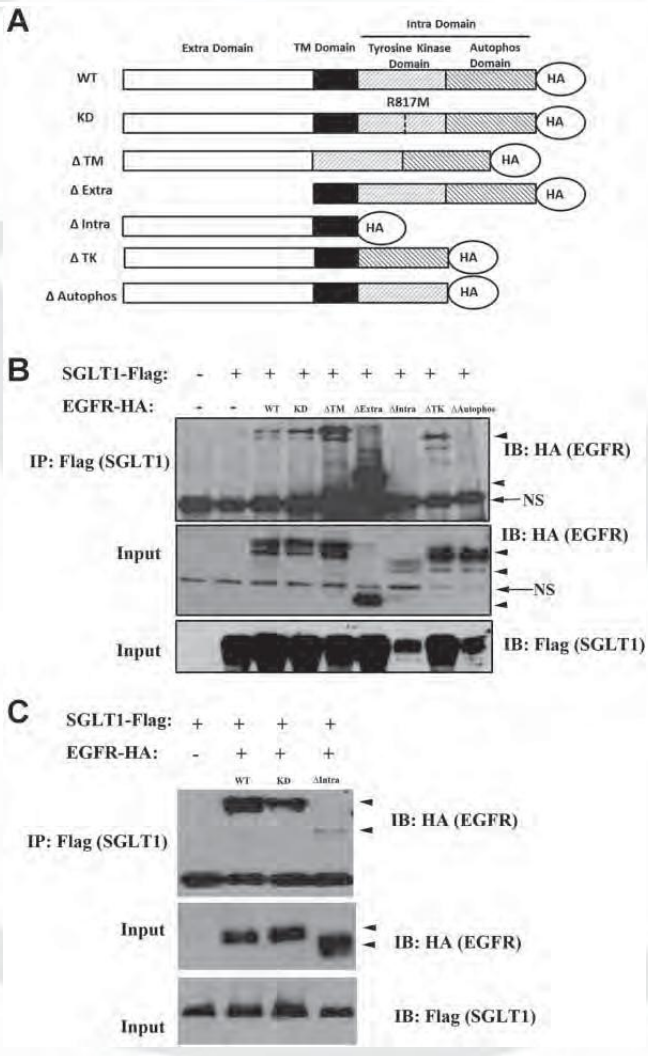

Fig. 1. The autophosphorylation domain of EGFR is required for its interaction with SGLT1. A: Schematic diagram of constructs of human EGFR used in this study: WT, wild-type EGFR; KD, kinase dead EGFR (R817M); DTM, transmembrane domain deletion (645^670aa); DExtra, extracellular domain deletion (1^644aa); DIntra, intracellular domain deletion (671^1210aa); DTK, tyrosine kinase domain deletion (670^977aa); DAutophos, autophosphorylation domain deletion (978^1210aa). B: Deletion of the entire intracellular domain or the autophosphorylation domain of EGFR significantly reduced its interaction with SGLT1. C: By increasing the expression level of the DIntra-EGFR, the DIntra-EGFR was co-precipitated with SGLT1. Immunoprecipitation coupled Western blot analysis of interactions between mutated EGFRs and SGLT1. IP, immunoprecipitation; IB, immunoblot. Input, expression levels of indicated exogenous proteins in HEK293 whole cell lysates used for the IP. EGFR bands are indicated by arrowheads. Nonspecific bands (NS) are indicated by arrows.

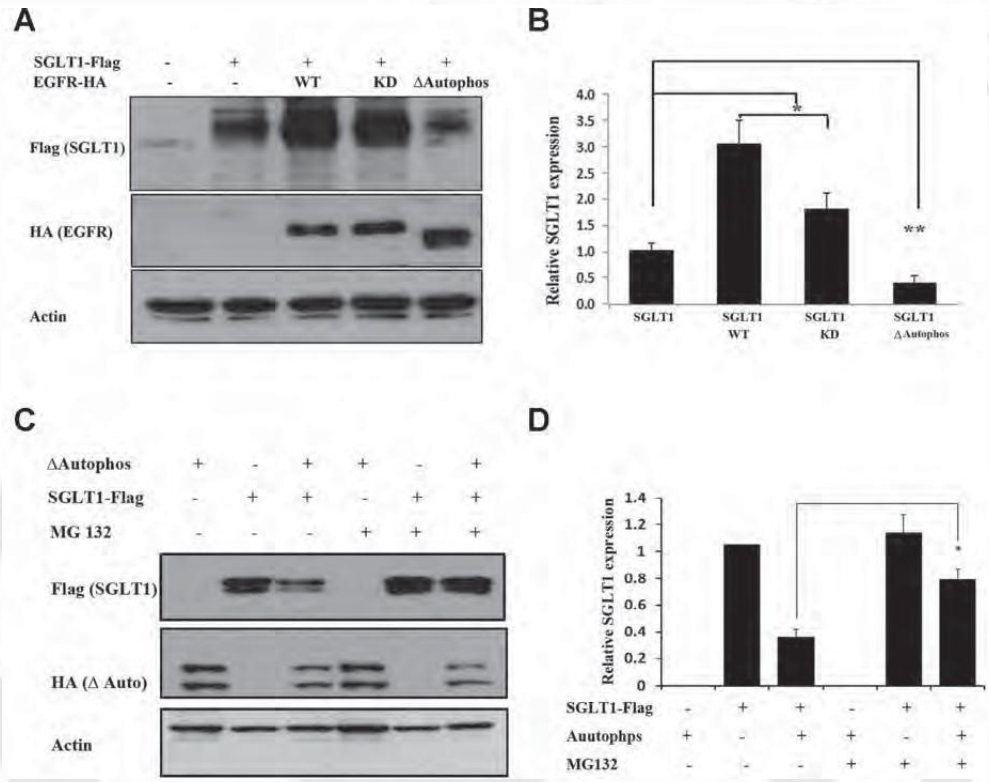

Fig. 2. The autophosphorylation domain of EGFR is required to prevent proteasome mediated SGLT1 degradation. A: Western blot analysis of expression levels of SGTL1 in HEK293 cells co-transfected with the WT-EGFR, the KD-EGFR, and the DAutophos-EGFR. The same amounts of DNA plasmids of SGLT1 and EGFRs were used in each group of treatments. Control cells were transfected with the same amount DNA of the empty vector. Actin was used as loading control. B: Densitometric quantification of bands in the Western blot of A. Asterisk marks indicate statistic significance between the linked representative group from triplicate experiments. C: Proteasome inhibitor MG132 blocked the down-regulation of SGLT1 by DAutophos-EGFR. Actin was used as a loading control. D: Densitometric quantification of bands in the Western blot of A. Asterisk marks indicate statistic significance between the linked representative group from triplicate experiments.

equal amount of plasmids of the flagged SGLT1 and these HA tagged EGFRs into HEK293 cells, immunoprecipitated SGLT1 using anti-flag antibodies, and performed WB analyses for HA tagged EGFRs. It was found that deletion of the autophosphorylation domain of EGFR completely abolished its interaction with SGLT1 (Fig. 1B). Under these experimental conditions, the DIntra-EGFR was not co-precipitated with SGLT1, which might be due to the expression level of the DIntra-EGFR was much lower than the other forms (Fig. 1B). To increase the expression level of the DIntra-EGFR, we increased the amount of plasmid cDNA of DIntra-EGFR by threefold for co-transfection. We found that the DIntra-EGFR was co-precipitated with SGLT1, however to a much less extent as compared with the WT-EGFR and the KD-EGFR that were expressed at a comparable level (Fig. 1C). These data indicate that the Autophos domain of EGFR is the major SGLT1 interacting domain, however the extracellular domain containing the transmembrane domain of EGFR, the DIntra-EGFR, can weakly interact with SGLT1.

The Autophosphorylation Domain of EGFR Is Required to Prevent Proteasome-Mediated SGLT1 Degradation

To determine whether the SGLT1-interacting domain of EGFR is required to sustain the stability of SGLT1, we measured the expression level of SGLT1 co-transfected with the WT-EGFR, the KD-EGFR and the DAutoPhos-EGFR into HEK293 cells. As shown in Figures Figure 2A and Figure 3B, the level of SGLT1 in the WT-EGFR and the KD-EGFR transfected cells is much higher than that in the control vector or DAutoPhos-EGFR transfected cells, suggesting the autophosphorylation domain of EGFR is needed to maintain the expression level of SGLT1. In addition, the level of SGLT1 in the DAutoPhos-EGFR transfected cells was also significantly lower than that of the control cells, suggesting that loss of interaction with EGFR may promote down-regulation of SGLT1. To determine whether proteasome is involved in loss of interaction with EGFR induced down-regulation of SGLT1, we treated SGLT1 and DAutoPhos-EGFR co-

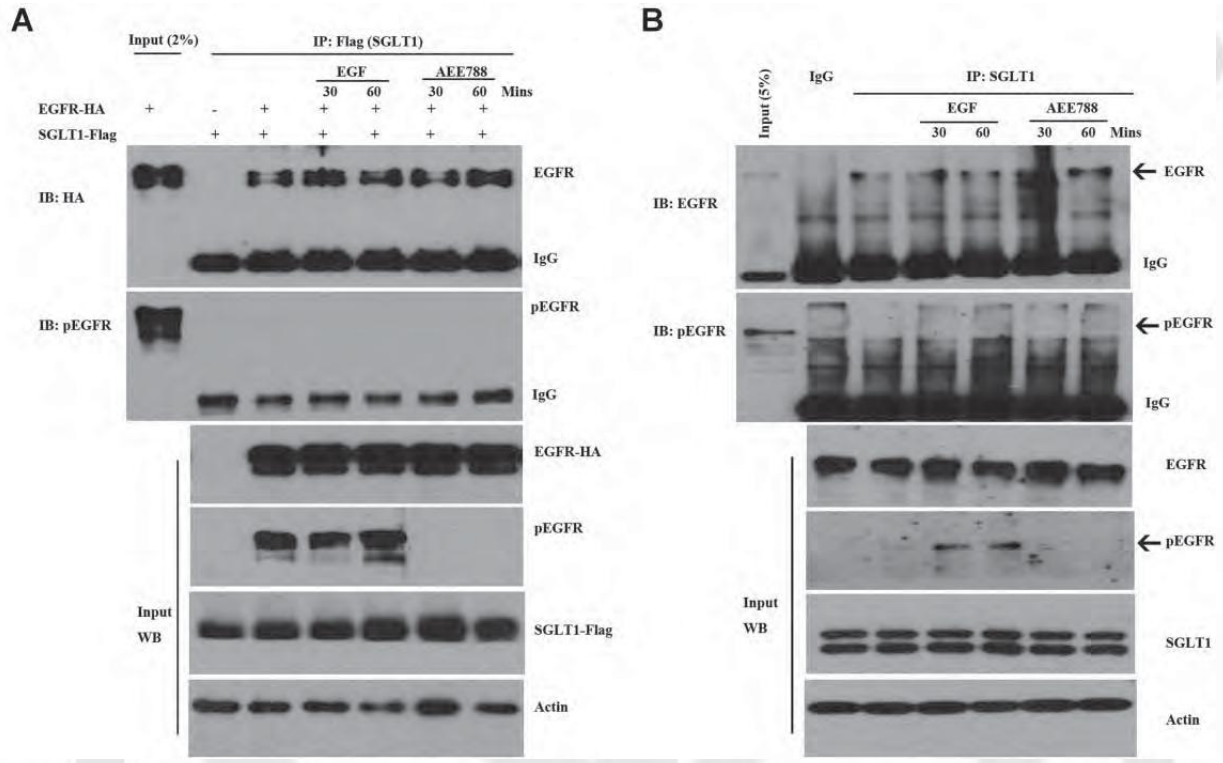

Fig. 3. EGFR^SGLT1 interaction is irresponsive to modulators of EGFR's tyrosine kinase. A: Immunoprecipitation coupled Western blot analysis of interactions between EGFR-HA and SGLT1-Flag in HEK293 cells treated with EGF or AEE788. EGFR, total EGFR; pEGFR, phosphorylated EGFR; IP, immunoprecipitation; IB, immunoblot. Input, expression levels of indicated exogenous proteins in HEK293 whole cell lysates used for the IP. B: Immunoprecipitation coupled Western blot analysis of interactions between endogenous EGFR and SGLT1 in PC3 cells treated with EGF or AEE788. EGFR, total EGFR; pEGFR, phosphorylated EGFR; IP, immunoprecipitation; IB, immunoblot. Input, expression levels of indicated exogenous proteins in HEK293 whole cell lysates used for the IP.

transfected HEK293 cells with a proteasome inhibitor, MG132. As shown in Figure 3C,D, MG132 inhibited the down-regulation of SGLT1 in DAutoPhos-EGFR transfected cells, suggesting the proteasome machinery is involved in loss of interaction with EGFR induced SGLT1 down-regulation.

EGFR^SGLT1 Interaction Is Irresponsive to Modulators of EGFR Tyrosine Kinase

Knowing that the tyrosine kinase activity of EGFR is not required for its interaction with SGLT1 (Fig. 1), we sought to determine the effects of EGFR ligand and its tyrosine kinase inhibitors on its interaction with SGLT1. We treated WT-EGFR and SGLT1 co-transfected HEK293 cells with either EGF or an EGFR tyrosine kinase inhibitor, AEE788. We then immunoprecipitated SGLT1 and measured the levels of EGFR that were co-immunoprecipitated with SGLT1. As shown in Figure 3A, neither EGF nor AEE788 affected EGFR–SGLT1 interaction and the EGFR co-precipitated with SGLT1 was not phosphorylated. To further determine the effects of EGF and AEE788 on endogenous EGFR–SGLT1 interaction and the phosphorylation status of endogenous EGFR that interacts with SGLT1, we immunoprecipitated the endogenous SGLT1 of PC3 cells treated with EGF or AEE788 and measured the phosphorylation status of the EGFR co-precipitated with SGLT1. We found that neither EGF nor AEE788 affected the EGFR–SGLT1 interaction and the endogenous SGLT1 interacting EGFR was not phosphorylated either (Fig. 3B). These results suggest that the EGFR–SGLT1 interaction is irresponsive to modulators of EGFR tyrosine kinase activity.

EGFR and SGLT1 Co-Localize in Prostate Cancer Tissues and Inhibition of SGLT1 by a SGLT1 Inhibitor Sensitized Prostate Cancer Cells to EGFR Inhibitors

To determine the clinical relevance of EGFR–SGLT1 interaction, we performed immunofluorescent co-staining of EGFR and SGLT1 on a tissue microarray of prostate cancers (n ¼ 44). In all the EGFR-positive cancer samples (n ¼ 41), we found SGLT1 co-localized with EGFR in cancer cells but not the stromal cells

(Fig. 4A). These data suggest that EGFR–SGLT1 interaction may contribute to the pathogenesis of prostate cancer.

It is known that an increase in glucose levels can activate EGFR [26], that SGLT1 is overexpressed in prostate cancer tissues [23], and that prostate cancer is resistant to EGFR inhibitors [9,10]. We speculated that SGLT1 and EGFR may synergistically promote prostate cancer growth. To test whether inhibition of SGLT1 can sensitize prostate cancer cells to EGFR inhibitors, we treated prostate cancer cell lines, PC3 and LNCaP (both positive for EGFR and SGLT1) (Fig. 4B), with EGFR tyrosine kinase inhibitors, Gefitnib and Erlotinib, in the presence/absence of a SGLT1 inhibitor, Phlorizin [27], and determined the growth inhibitory effects of the treatments. It was found that

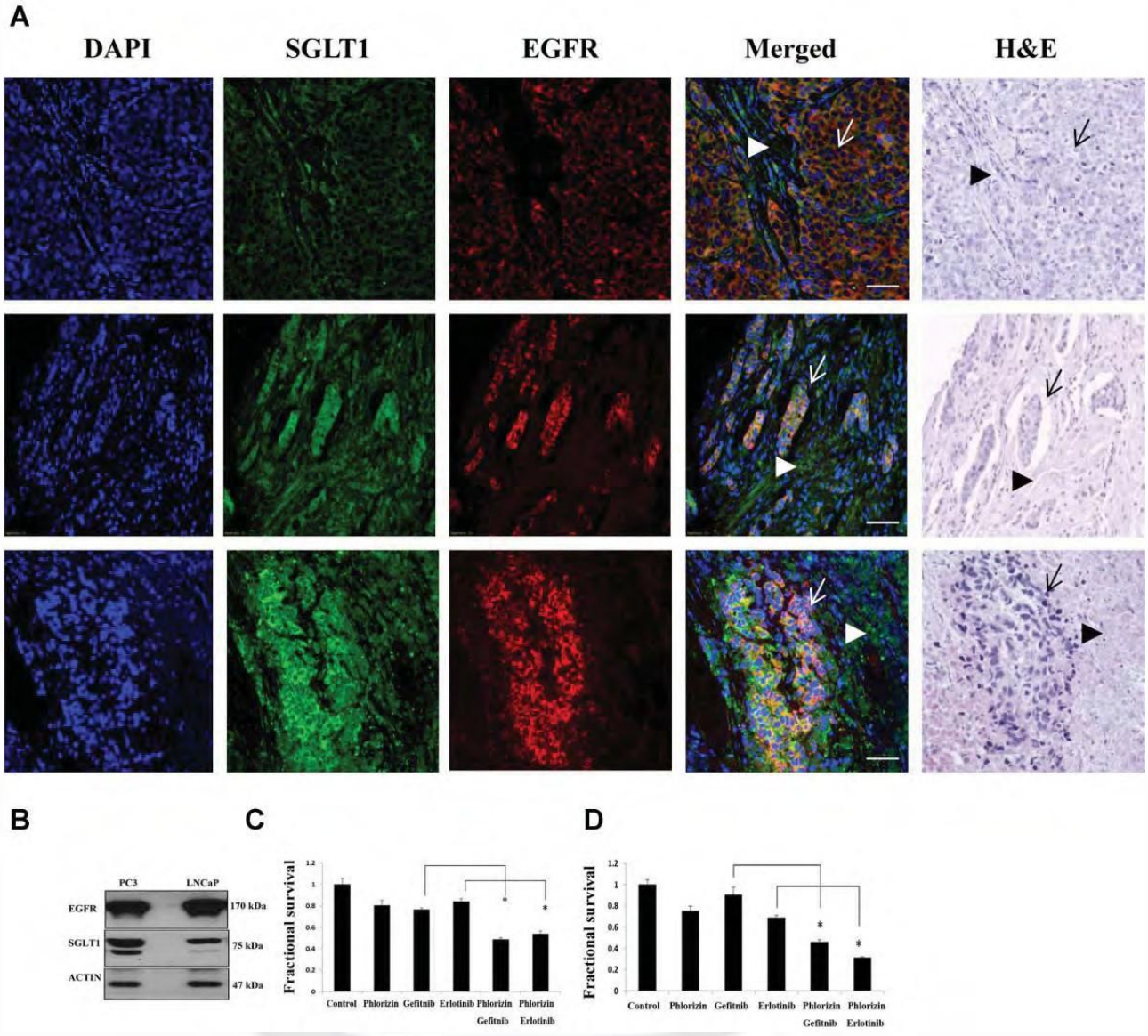

Fig. 4. Co-localization of EGFR and SGLT1 in prostate cancer tissues by immunofluorescent co-staining and inhibition of SGLT1 by a SGLT1 inhibitor sensitized prostate cancer cells to EGFR inhibitors. A: Results of three representative prostate cancer tissues from a prostate cancer tissue array are presented. Co-localization of SGLT1 (green) and EGFR (red) are in colors of orange or yellow (arrows). H&E, hematoxylin and eosin staining. Note: The stromal cells (arrow heads) are positive for SGLT1 but negative for EGFR. Bar ¼ 100 mm. B: Western analysis of the expressions of endogenous EGFR and SGLT1 in PC3 and LNCaP cells. C: MTT assay for the effect of Phlorizin on the growth inhibitory effect of Gefitinib and Erlotinib on LNCaP cells. D: MTT assay for the effect of Phlorizin on the growth inhibitory effect of Gefitinib and Erlotinib on LNCaP cells. Cells were treated with SGLT1 inhibitor Phlorizin (50 mM) with/without EGFR inhibitors (Gefitinib, 20 mM; Erlotinib, 20 mM) for 48 hr before subjected to MTT assay. The OD value of control cells was artificially set as 1. All experiments were repeated at least three times. Asterisks indicate statistical significance between linked groups.

Phlorizin was additive to the growth inhibitory effects of Gefitnib and Erlotinib (Fig. 4C,D).

DISCUSSION

Previously, using EGFR's extracellular domain and intracellular domain that does not contain the TM domain of EGFR, we reported that SGLT1 interacted stronger with the extracellular domain of EGFR than the intracellular domain of EGFR [14]. To further characterize the EGFR–SGLT1 interaction at the plasma membrane, we included the TM domain in to the constructs of truncated EGFRs. We found that the TM containing intracellular domain of EGFR, especially the autophosphorylation domain, interacted with SGLT1 much stronger than the extracellular domain of EGFR. The discrepancy between current data and the data shown in the previous report [14] is likely due to the lack of TM domain in the intracellular domain construct of EGFR used in the previous study. The findings that the autophosphorylation domain of EGFR interacts with SGLT1 and this interaction is independent of activation/inactivation of EGFR (Figs. 1–3) have significant implications. It has been well characterized that, upon phosphorylation of tyrosines within the autophosphorylation domain, the autophosphorylation domain serves as a major docking site for recruitment of adaptor/effector proteins that transactivate downstream signalings [28]. Our present data indicate that the autophosphorylation domain of EGFR can also function as a protein–protein interacting domain independent of EGFR tyrosine kinase activity. These findings further support that EGFR owns pro-survival functions independent of its tyrosine kinase activity. In other words, EGFR may exist as a tyrosine kinase-responsive and a tyrosine kinase-irresponsive status. Upon activation by EGFR's ligands, the autophosphorylation domain of the kinase-responsive EGFR is phosphorylated and recruits effectors to trigger downstream signals. However, the kinase-irresponsive EGFR constantly interacts with proteins regardless of the presence of EGFR ligands and activation or inactivation of its tyrosine kinase. SGLT1 is one such protein that can bind to and keep EGFR in its kinase-irresponsive status.

The co-localization of EGFR with SGLT1 in prostate cancer tissues strongly indicates that the EGFR–SGLT1 interaction is relevant to cancer metabolism. In the clinic, EGFR tyrosine kinase inhibitors did not produce therapeutic effects for prostate cancer [9,10]. Considering the fact that EGFR expression correlates with disease progression of prostate cancer and the clinical unresponsiveness of prostate cancers to EGFR tyrosine kinase inhibitors, we propose that EGFR may contribute to the disease progression of prostate cancer independent of its tyrosine kinase activity. Previously, we have found that prostate cancer tissues have increased expression of SGLT1 [23], loss of EGFR protein but not its tyrosine kinase activity sensitized prostate cancer cells to chemotherapeutic agent [29], and loss of EGFR-induced autophagic cell death was mediated by down-regulation of SGLT1 protein [14]. These data suggest that EGFR can promote prostate cancer progression via stabilizing SGLT1 to sustain the high demand of glucose by late stage cancer cells. This possibility is supported by our data that treatment of prostate cancer cells with a SGLT1 inhibitor sensitized cancer cells to EGFR inhibitors (Fig. 5[Q3]), as well as data demonstrating that overexpression of SGLT1 protected renal epithelial cells [30] and intestinal epithelial cells [31] from apoptosis.

The deletion of the SGLT1 interacting domain in EGFR promoted the down-regulation of SGTL1 via the proteasome machinery (Fig. 2), suggesting that disruption of EGFR–SGLT1 interaction in EGFR-positive cancer cells may lead to down-regulation of SGLT1. Given that knocking down SGLT1 by shRNA resulted in autophagic cell death of prostate cancer cells [14], it is suggested that the EGFR–SGLT1 interaction might be a novel target to improve EGFR-based therapy for prostate cancer.

ACKNOWLEDGMENTS

The authors thank Dr. Isaiah J. Fidler for constructive comments on the manuscript and Lola Lopez for expert assistance with the article preparation. Z. W. is supported in part by grants from the American Cancer Society (RSG-09-206-01), the Department of Defense Prostate Cancer Research Program (W91ZSQ8334N607), and a startup fund from the University of Houston.

REFERENCES

1. Hynes NE, Lane HA. ERBB receptors and cancer: The complexity of targeted inhibitors. Nat Rev Cancer 2005;5(5):341–354.
2. Weiss J. First line erlotinib for NSCLC patients not selected by EGFR mutation: Keep carrying the TORCH or time to let the flame die? Transl Lung Cancer Res 2012;1(3):219–223.
3. Cohen SJ, Ho L, Ranganathan S, Abbruzzese JL, Alpaugh RK, Beard M, Lewis NL, McLaughlin S, Rogatko A, Perez-Ruixo JJ, Thistle AM, Verhaeghe T, Wang H, Weiner LM, Wright JJ, Hudes GR, Meropol NJ. Phase II and pharmacodynamic study of the farnesyltransferase inhibitor R115777 as initial therapy in patients with metastatic pancreatic adenocarcinoma. J Clin Oncol 2003;21(7):1301–1306.
4. Dancey JE, Freidlin B. Targeting epidermal growth factor receptor—Are we missing the mark? Lancet 2003;362(9377): 62–64.

5. Hernes E, Fossa SD, Berner A, Otnes B, Nesland JM. Expression of the epidermal growth factor receptor family in prostate carcinoma before and during androgen-independence. Br J Cancer 2004;90(2):449–454.
6. Pu YS, Hsieh MW, Wang CW, Liu GY, Huang CY, Lin CC, Guan JY, Lin SR, Hour TC. Epidermal growth factor receptor inhibitor (PD168393) potentiates cytotoxic effects of paclitaxel against androgen-independent prostate cancer cells. Biochem Pharmacol 2006;71(6):751–760.
7. Sherwood ER, Lee C. Epidermal growth factor-related peptides and the epidermal growth factor receptor in normal and malignant prostate. World J Urol 1995;13(5):290–296.
8. Zellweger T, Ninck C, Bloch M, Mirlacher M, Koivisto PA, Helin HJ, Mihatsch MJ, Gasser TC, Bubendorf L. Expression patterns of potential therapeutic targets in prostate cancer. Int J Cancer 2005;113(4):619–628.
9. Canil CM, Moore MJ, Winquist E, Baetz T, Pollak M, Chi KN, Berry S, Ernst DS, Douglas L, Brundage M, Fisher B, McKenna A, Seymour L. Randomized phase II study of two doses of gefitinib in hormone-refractory prostate cancer: A trial of the National Cancer Institute of Canada-Clinical Trials Group. J Clin Oncol 2005;23(3):455–460.
10. Gross M, Higano C, Pantuck A, Castellanos O, Green E, Nguyen K, Agus DB. A phase II trial of docetaxel and erlotinib as first-line therapy for elderly patients with androgen-independent prostate cancer. BMC Cancer 2007;7:142.
11. Threadgill DW, Dlugosz AA, Hansen LA, Tennenbaum T, Lichti U, Yee D, LaMantia C, Mourton T, Herrup K, Harris RC, et al. Targeted disruption of mouse EGF receptor: Effect of genetic background on mutant phenotype. Science 1995;269(5221):230–234.
12. Luetteke NC, Phillips HK, Qiu TH, Copeland NG, Earp HS, Jenkins NA, Lee DC. The mouse waved-2 phenotype results from a point mutation in the EGF receptor tyrosine kinase. Genes Dev 1994;8(4):399–413.
13. Ewald JA, Wilkinson JC, Guyer CA, Staros JV. Ligand- and kinase activity-independent cell survival mediated by the epidermal growth factor receptor expressed in 32D cells. Exp Cell Res 2003;282(2):121–131.
14. Weihua Z, Tsan R, Huang WC, Wu Q, Chiu CH, Fidler IJ, Hung MC. Survival of cancer cells is maintained by EGFR independent of its kinase activity. Cancer Cell 2008;13(5):385–393.
15. Wright EM, Loo DD, Hirayama BA. Biology of human sodium glucose transporters. Physiol Rev 2011;91(2):733–794.
16. Castaneda-Sceppa C, Castaneda F. Sodium-dependent glucose transporter protein as a potential therapeutic target for improving glycemic control in diabetes. Nutr Rev 2011;69(12):720–729.
17. Hanahan D, Weinberg RA. Hallmarks of cancer: The next generation. Cell 2011;144(5):646–674.
18. Ganapathy V, Thangaraju M, Prasad PD. Nutrient transporters in cancer: Relevance to Warburg hypothesis and beyond. Pharmacol Ther 2009;121(1):29–40.
19. Lai B, Xiao Y, Pu H, Cao Q, Jing H, Liu X. Overexpression of SGLT1 is correlated with tumor development and poor prognosis of ovarian carcinoma. Arch Gynecol Obstet 2012;285(5):1455–1461.
20. Hanabata Y, Nakajima Y, Morita K, Kayamori K, Omura K. Coexpression of SGLT1 and EGFR is associated with tumor differentiation in oral squamous cell carcinoma. Odontology 2012;100(2):156–163.
21. Guo GF, Cai YC, Zhang B, Xu RH, Qiu HJ, Xia LP, Jiang WQ, Hu PL, Chen XX, Zhou FF, Wang F. Overexpression of SGLT1 and EGFR in colorectal cancer showing a correlation with the prognosis. Med Oncol 2011;28(Suppl. 1):S197–S203.
22. Casneuf VF, Fonteyne P, Van Damme N, Demetter P, Pauwels P, de Hemptinne B, De Vos M, Van de Wiele C, Peeters M. Expression of SGLT1, Bcl-2 and p53 in primary pancreatic cancer related to survival. Cancer Invest 2008;26(8):852–859.
23. Blessing A, Xu L, Gao G, Bollu RL, Ren J, Li H, Wu X, Su F, Huang W-C, Hung MC, Huo L, Palapattu SG, Weihua Z. Sodium/glucose co-transporter 1 expression increases in human diseased prostate. J Cancer Sci Ther 2012;4(9):306–312.
24. Lee ST, Lawrentschuk N, Scott AM. PET in prostate and bladder tumors. Semin Nucl Med 2012;42(4):231–246.
25. Oyama N, Akino H, Suzuki Y, Kanamaru H, Sadato N, Yonekura Y, Okada K. The increased accumulation of [18F]fluorodeoxyglucose in untreated prostate cancer. Jpn J Clin Oncol 1999;29(12):623–629.
26. Han L, Ma Q, Li J, Liu H, Li W, Ma G, Xu Q, Zhou S, Wu E. High glucose promotes pancreatic cancer cell proliferation via the induction of EGF expression and transactivation of EGFR. PLoS ONE 2011;6(11):e27074.
27. Ehrenkranz JR, Lewis NG, Kahn CR, Roth J. Phlorizin: A review. Diabetes Metab Res Rev 2005;21(1):31–38.
28. Bazley LA, Gullick WJ. The epidermal growth factor receptor family. Endocr Relat Cancer 2005;12(Suppl. 1):S17–S27.
29. Xu S, Weihua Z. Loss of EGFR induced autophagy sensitizes hormone refractory prostate cancer cells to adriamycin. Prostate 2011.
30. Ikari A, Nagatani Y, Tsukimoto M, Harada H, Miwa M, Takagi K. Sodium-dependent glucose transporter reduces peroxynitrite and cell injury caused by cisplatin in renal tubular epithelial cells. Biochim Biophys Acta 2005;1717(2):109–117.
31. Yu LC, Huang CY, Kuo WT, Sayer H, Turner JR, Buret AG. SGLT-1-mediated glucose uptake protects human intestinal epithelial cells against Giardia duodenalis-induced apoptosis. Int J Parasitol 2008;38(8–9):923–934.

Cancer
Science & Therapy

Blessinget al., J Cancer Sci Ther 2012, 4.9
http://dx.doi.org/10.4172/1948-5956.1000159

Research Article Open Access

Sodium/Glucose Co-transporter 1 Expression Increases in Human Diseased Prostate

Alicia Blessing[1], Lei Xu[1], Guang Gao[1], Lakshmi Reddy Bollu[1], Jiangong Ren[1], Hangwen Li[2], Xuefeng Wu[1], Fei Su[1], Wei-Chien Huang[3], Mien-Chie Hung[3,4], Lei Huo[5], Ganesh S Palapattu[2] and Zhang Weihua[1]*

[1]*Department of Biology and Biochemistry, University of Houston, Houston, TX, 77204, USA*
[2]*Department of Urology, Methodist Hospital Research Institute, Houston, TX, 77030, USA*
[3]*Center for Molecular Medicine and Graduate Institute of Cancer Biology, China Medical University Hospital, Taichung 404, Taiwan*
[4]*Department of Molecular and Cellular Oncology, The University of Texas MD Anderson Cancer, Center, Houston, TX 77030, USA*
[5]*Department of Pathology, The University of Texas MD Anderson Cancer Center, Houston, TX, 77030, USA*

Abstract

Sodium/glucose co-transporter 1 (SGLT1) is an active glucose transporter that takes up glucose into cells independent of the extracellular concentration of glucose. This transporter plays a critical role in maintaining glucose homeostasis at both physiological and pathological levels. The expression level of SGLT1 in normal and diseased human prostatic tissue has not been determined. We produced two rabbit polyclonal antibodies against human SGLT1, one each for immunohistochemical and Western blot analyses, and characterized the expression of SGLT1 in human prostate tissues: normal prostate (n=3), benign prostatic hyperplasia (BPH) (n=53), prostatic intraepithelial neoplasia (PIN) (n=9), and prostate cancer (PCa) (n=44). In normal prostate tissue, SGLT1 was weakly expressed exclusively in the epithelium. The transporter was significantly increased in the basal cells and stromal cells of BPH, increased in the epithelial cells of PIN, and frequently overexpressed in stromal cells and universally overexpressed in the tumor cells of PCa. The pattern of expression was shown as membranous/cytoplasmic staining in low-grade cancer cells and nuclear envelope staining in high-grade cancer cells. The SGLT1-positive stromal cells of BPH and PCa tissues were negative for tenascin, a marker of reactive stromal cells. We concluded that SGLT1 is up-regulated in BPH and PCa, and SGLT1 may serve as a potential therapeutic target for treating these prostate disorders.

Keywords: SGLT1; Prostate; Prostate cancer; Benign prostatic hyperplasia

Introduction

Influx of glucose into cells is carried out by two main classes of glucose transporters, the facilitative glucose transporters (GLUTs) and the active sodium/glucose co-transporters (SGLTs) [1]. GLUTs mediate a concentration-dependent and energy-independent bidirectional process of glucose transport. In contrast, SGLTs mediate an active Na^+ gradient–dependent glucose uptake regardless of the extracellular glucose concentration [2,3]. The SGLT family consists of 3 members, SGLT1, SGLT2, and SGLT3 [1]; the last may function as a glucose sensor rather than a transporter [4].

Increased glucose uptake and GLUT expression are associated with pathological conditions, such as hypoxia, inflammation, and neoplasia. Hypoxia induces GLUT1 expression in neurons [5,6] and chondrocytes [6], and inflammation up-regulates GLUT1 in macrophages [7] and vascular endothelial cells [8]. GLUT1 is often induced in many cancers, including those of the breast, cervix, esophagus, lung, and liver [9]. Increased expressions of SGLT1 have been found in oral cancer [10], colorectal cancer [11], pancreatic cancer [12], and ovarian cancer [13].

Normal prostatic epithelium is not active in glucose metabolism [14]. However, glucose uptake has often been observed with high-grade prostate cancer (PCa) [15] hinting at an association between altered glucose metabolism and the pathogenesis of PCa. Yet several studies have found significantly decreased levels of GLUT expression in PCa [16,17]. The glucose transporter or transporters that are involved in the increased glucose uptake observed in PCa remain to be investigated.

To explore the possibility of a role for SGLT in pathogenesis of prostate diseases, we produced and characterized two rabbit polyclonal antibodies against human SGLT1 to examine its expression levels in human prostate tissues including normal, benign prostate hyperplasia (BPH), prostatic intraepithelial neoplasia (PIN), and PCa.

Materials and Methods

Antibody production and purification

Two peptides, CIETQVPEKKKGIFRR and CLRNSKEERIDLDAE, corresponding to amino acids 588-604 and 563-576 of human SGLT1 were used to raise rabbit polyclonal antibodies suitable for immunohistochemical analysis (SGLT1-IHC) and Western blotting (SGLT1-WB) respectively.

HiTrap affinity columns (General Electric, Uppsala, Sweden) were used to purify the SGLT1 antibodies from SGLT1 antiserum. To purify the antibody, the columns were coupled with the antigenic peptide at a concentration of 1 mg/mL in coupling buffer (0.2 M $NaHCO_3$, 0.5 M NaCl, pH=8.3) for 30 minutes at room temperature. The column was then exposed to buffer A (0.5 M ethanolamine, 0.5 M NaCl, pH=8.3) and buffer B (0.1 M acetate, 0.5 M NaCl, pH=4) 3 times. Five hundred

***Corresponding author:** Zhang Weihua, PhD, Assistant Professor, Department of Biology and Biochemistry, College of Natural Sciences and Mathematics, University of Houston, Houston, TX 77204-5001, Office: HSC358, USA, Tel. 713-743-8382; E-mail: wzhang13@uh.edu

Received June 30, 2012; **Accepted** August 28, 2012; **Published** August 30, 2012

Citation: Blessing A, Xu L, Gao G, Bollu LR, Ren J, et al. (2012) Sodium/Glucose Co-transporter 1 Expression Increases in Human Diseased Prostate. J Cancer Sci Ther 4: 306-312. doi:10.4172/1948-5956.1000159

microliters of the pre-immune serum and 500 µL of the antiserum were diluted in binding buffer (0.2 M NaH_2PO_4, pH=7.0) and passed through the column. The bound antibodies were eluted with 3 mL of elution buffer (1 M glycine-HCl, pH=2.7). The elutant was immediately neutralized with neutralizing buffer (1 M Tris-HCl, pH=9.0), and 0.02% Na_3N was added to the purified antibody for long-term storage.

Cell culture

PC3, PC3-MM2, LNCaP, HCT116, and HEK293T were from our laboratory cell stocks. All types of cells were cultured in Dulbecco's modified Eagle's medium) (Invitrogen, Carlsbad, CA) and supplemented with 5.5 mM glucose, 10% fetal bovine serum, and 1% penicillin/streptomycin. Cells were cultured at 37°C with 5% CO_2.

Plasmid construction

Human SGLT1 cDNA was amplified from a cDNA library using a pair of primers, GCTGCCACCATGGACAGTAG and CAGCAAAAGGTAGGACTCAGG, corresponding to the 5′ and 3′ UTR of SGLT1. A second round of polymerase chain reaction was performed using a pair of nested primers, TGAGTCGACGGCAAAATATGCATGGCAAAAGACAGCCACGGTCACC and ATAGAATTCATGGACAGTAGCACCTGGAGCCCCAAGACCA. The polymerase chain reaction product of SGLT1 was cloned into a PXF2F expression vector between the SalI and EcoRI sites, which produced a SGLT1 cDNA with a FLAG tag at both the N-terminus and the C-terminus. The construct was confirmed by sequencing. The tagging at both ends allows the protein to be expressed at a stable level in the absence of epidermal growth factor receptor (EGFR) and was used as a positive control for antibody characterization.

The U6 promoter-driven small interfering (shRNA) vector with green fluorescent protein (GFP) expression (pRNAT-U6.1/Neo; GenScript) was used to express shRNA against SGLT1. The target sequence for SGLT1 shRNA was TCTTCCGCATCCAGGTCAAT. The negative control shRNA sequence was GAACAATGTTGACCAGGTGA.

shRNA knockdown, RT-PCR and western blotting

Whole-cell lysates of intact cells were transfected with vectors expressing FLAG-tagged SGLT1 in combination with vectors expressing SGLT shRNA or its corresponding scrambled control. At the time of transfection, cells were cultured in their respective media without the supplemented 1% penicillin/streptomycin. Six hours post-transfection, the media were replaced with normally formulated media. At 48 hours after transfection, one set of cells were used for RNA isolation and RT-PCR determination of SGLT1 mRNA (primers are: 5′-TGGCAGGCCGAAGTA-TGGTGT-3′ and 5′-ATGAATATGGCCCCCGAGAAGA-3′) and beta actin as an internal control (5′-ATCTGGCACCACACCTTCTACAATG-3′ and 5′-CGTCATACTC-CTGCTTGCTG-3′). The RT-PCR reaction program was set to 50°C for 1 hr and 94°C for 5 min, followed by 30 cycles of 94°C for 40 s, 56°C for 40 s, and 72°C for 50 s with an extension at 72°C for 10 min. The PCR products were analyzed with a 1% agarose gel stained with ethidium bromide and visualized under ultraviolet light. Another set of cells were lysed for 30 minutes on ice in RIPA buffer (Sigma Aldrich, St. Louis, MO) supplemented with protease and phosphatase inhibitors for Western Blot and immunoprecipitation assays. The concentrations of the protein samples were measured using a Qubit flourometer (Invitrogen), and equal amounts of protein samples were loaded onto a 10% SDS-PAGE gel and transferred to a polyvinylidine fluoride membrane. Membranes were incubated in 5% milk to block the non-specific binding sites for 30 minutes and then in optimized concentrations of SGLT1-WB or primary anti-FLAG antibody (Santa Cruz Biotechnology, Santa Cruz, California) at 4°C overnight. After being washed with 3x phosphate-buffered saline (PBS), membranes were incubated with horseradish peroxidase–conjugated secondary antibodies (Santa Cruz Biotechnology) at 1:3000 dilutions for 1 hour at room temperature. Luminescent signals were detected using an enhanced luminescence kit (Pierce ThermoScientific, Rockford, IL) and exposed to X-ray film (VWR, Bridgeport, NJ).

Immunoprecipitatioin

HEK 293 cells were transfected with double flagged SGLT1. After 24 hours of post transfection cells were washed in 1X phosphate buffered solution and lysed with RIPA buffer (50 mM Tris-HCl, pH 8.0, with 150 mM sodium chloride, 1.0% Igepal CA-630 (NP-40), 0.5% sodium deoxycholate, and 0.1% sodium dodecyl sulfate), supplemented with ptotease inhibitors cock tail, for 6 hours at 4°C on a shaker. The cell lysates were then centrifuged for 2 minutes at 12000 rpm and 500 µgs of supernatants were incubated with 25 µl of sepharose protein A/G beads (Santa Crusz Biotechnology, Santa Cruz, CA, USA) conjugated with 500 ng anti-flag antibody (Sigma) for overnight. Samples were then centrifuged and washed with RIPA buffer three times before boiled in Laemmle buffer (Biorad, Hercules, CA, USA) and subjected to Western blot analysis using the SGLT1-WB antibody.

shRNA knockdown and immunocytochemical analysis

Vectors expressing SGLT shRNA or its corresponding scrambled control were transiently transfected into HCT116 cells cultured on collagen-coated glass coverslips using Lipofectamine 2000 (Invitrogen) in Opti-MEM (Invitrogen). At the time of transfection, cells were cultured in their respective media without the supplemented 1% penicillin/streptomycin. Six hours post-transfection, the media were replaced with normally formulated media. At 30 hours post-transfection, cells were fixed with 4% paraformaldehyde and permeabilized with 0.5% Triton X-100 (Sigma-Aldrich) in PBS.

Slides were blocked by incubating cells in normal goat serum for 1 hour followed by primary antibody against SGLT1 (1:200 in PBS) overnight at 4°C. After being washed, cells were exposed to Alexa Fluor 594 secondary antibody (1:200; Invitrogen) for 1 hour at room temperature. After three washes with PBS, coverslips were mounted on microscopic slides using 10 µl of VECTASHIELD mounting medium with 4',6-diamidino-2-phenylindole (DAPI) (Vector Laboratories, Burlingame, CA). Fluorescence images were captured and analyzed with a fluorescent Olympus microscope.

Tissue preparation

Paraffin-embedded tissue microarrays containing normal human tissues and human prostate tissues, BPH tissues, PIN tissues, and PCa tissues were purchased from Lifespan Biosciences (Seattle, WA). An additional five BPH tissue samples were obtained from the Methodist Hospital Research Institute's Department of Urology (Houston, TX) tissue bank under the approval of its institutional review board.

IHC analysis

Immunoperoxidase staining: For immunoperoxidase staining with diaminobenzidine labeling, tissue sections were deparaffinized in xylene and rehydrated in a graded series of alcohol and PBS. Antigen retrieval was performed using heated citrate buffer. Endogenous peroxidase activity was blocked with 3% hydrogen peroxide in

methanol. Samples were incubated in a blocking solution (5% donkey serum in PBS) for 1 hour at room temperature and then overnight at 4°C with the primary antibody against SGLT1 diluted in the blocking solution (1:200). After three washes in PBS, samples were incubated with a biotinylated goat anti-rabbit secondary antibody (1:500) for 1 hour at room temperature and then washed thoroughly. An ABC staining kit was used for chromogenesis. Slides were then briefly counterstained with hematoxylin and mounted.

Immunofluorescent co-staining: For immunofluorescent co-staining of SGLT1 and tenascin**,** tissue slides were co-incubated with the rabbit polyclonal antibody against SGLT1 (1:200 dilution, or with 1 mg/mL blocking peptides for the control) and a monoclonal anti-tenascin antibody (1:200) in PBS containing 10% donkey serum. After being washed three times with PBS, tissues were incubated with Alexa Fluor 488–conjugated donkey anti-rabbit immunoglobulin G, Alexa Flour 594–conjugated donkey anti-mouse immunoglobulin G, or both (Invitrogen) in PBS containing 10% donkey serum for 30 minutes at room temperature. The stained samples were then washed three times (5 minutes per wash) with PBS, also at room temperature. Fluorescence images were captured and analyzed with a confocal microscope (Olympus).

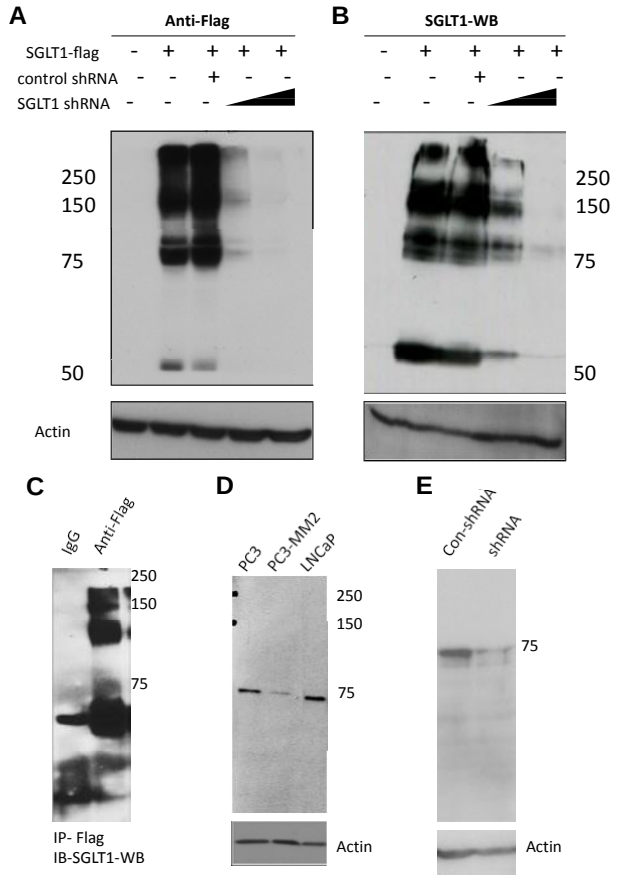

Figure 1: Characterization of the SGLT1-WB antibody by Western blot analysis. Detection of FLAG-tagged SGTL1 transiently transfected into HEK293T cells in combination with control shRNA or SGLT1 shRNA, using **A**, an anti-FLAG primary antibody or **B**, SGLT1-WB. **C**, WB detection of immunoprecipitated flagged SGLT1 expressed in HEK293 cells using the SGLT1-WB antibody. **D**, SGLT1 expression in PC3, PC3-MM2, and LNCaP cells. **E,** Detection of endogenous SGLT1 of PC3 cells transfected with control shRNA or SGLT1 shRNA, using SGLT1-WB. Actin was used as the loading control.

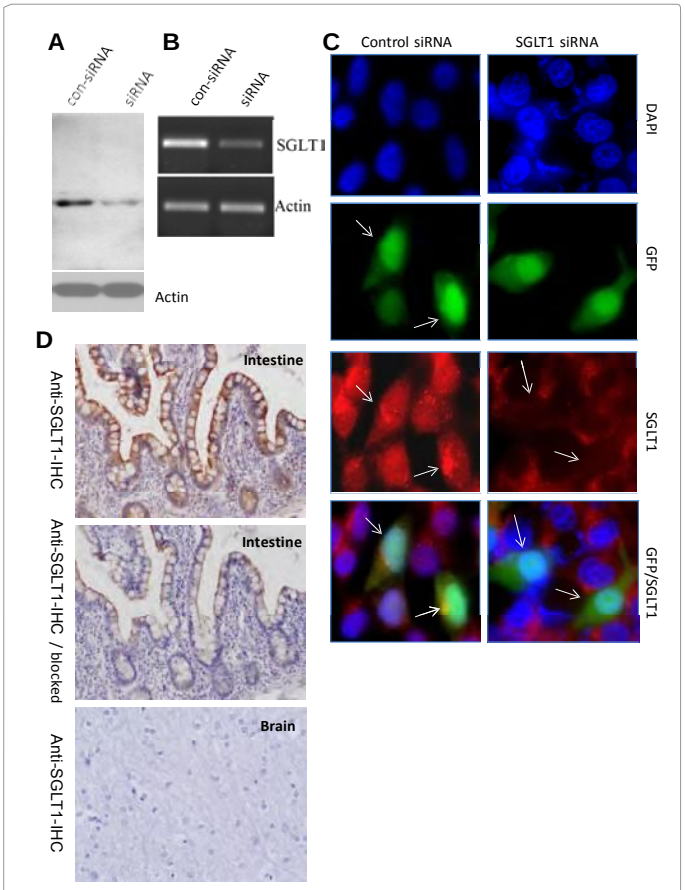

Figure 2: Characterization of the SGLT1-IHC antibody using HCT116 human colon cancer cells. **A**, Western blot analysis of endogenous SGLT1 in cells transfected with control shRNA or SGLT1 shRNA using the SGLT1-WB antibody, which was consistent with the changes of SGLT1 mRNA levels determined by RT-PCR **B**, Actin was used as internal controls. **C**, Immunocytochemical analysis of cells transfected with control shRNA or SGLT1 shRNA using SGLT1-IHC. Cells containing shRNA appear green (arrows) due to the expression of GPF under the control of an autonomous promoter and the SGLT1 signal is red. Nuclei are stained blue with DAPI. **D**, Immunohistochemical analysis of a human normal intestine sample using SGLT1-IHC with or without blocking peptides (1 mg/mL).

Results

Characterization of rabbit antibodies against human SGLT1

SGLT1-WB: The specificity of SGLT1-WB was characterized by the following experiments. First, we transiently transfected FLAG-tagged SGLT1 plasmids with either SGLT1 shRNA or control shRNA into HEK293T cells and determined the levels of FLAG-tagged SGLT1 of these cells by Western blotting using a primary antibody against FLAG. The flagged SGLT1 produced four major bands of >250, 150, 80, and 55 kDa, which were all substantially reduced only by the SGLT1 shRNA in a dose-dependent manner (Figure 1A). The >250 kDa and 150 kDa bands might be aggregates of overexpressed SGLT1. Because the exogenous SGLT1 was flagged at both the N- and C-termini, the expected molecular weight was 80 kDa. The 55 kDa band is likely degraded SGLT1. Using the same set of cell lysates, we detected the expression of SGLT1 in these cells using the SGLT1-WB primary antibody. The results were similar, will all four bands detected by

SGLT1-WB reduced by SGLT1 shRNA in a dose-dependent manner (Figure 1B). To further determine the specificity of the SGLT1-WB antibody, we performed an assay of immunoprecipitation coupled with Western blot (IP-WB) using the anti-flag antibody for IP and the SGLT1-WB for WB, and an irrelevant rabbit IgG as a negative control. As shown in Figure 1C, the immunoprecipitated flagged SGLT1 was detected by the SGLT1-WB antibody. We then determined the expression of endogenous SGLT1 in a panel of cell lines PC3, PC3-MM2, and LNCaP. SGLT1-WB detected a single band at the expected 75 kDa (endogenous SGLT1) in the PC3, PC3-MM2, and LNCaP lines (Figure 1D). To determine the specificity of the endogenous SGLT1 signal, we transiently transfected SGLT1 shRNA and its control shRNA into PC3 cells and determined the expression levels of the endogenous SGLT1 using SGLT1-WB. The SGLT1 signal was reduced by the addition of SGLT1 shRNA (Figure 1E). Taken together, these data suggest that SGLT1-WB is suitable for Western blot analysis.

SGLT1-IHC: To characterize the SGLT1-IHC antibody, we conducted two types of control experiments. First, we tested the specificity of this antibody by using immunocytochemical analysis on cells treated with control shRNA or SGLT1 shRNA. Because colon cancers express SGLT1 (11) we used colon cancer HCT116 cells as a positive control. The expression of SGLT1 in HCT116 cells treated with control shRNA or SGLT1 shRNA was first confirmed by Western blotting using the SGLT1-WB antibody (Figure 2A) and RT-PCR analysis of the SGLT1 mRNA (Figure 2B). Then we performed immunocytochemical staining using SGLT1-IHC with HCT116 cells. The shRNA expression vector expresses green fluorescent protein (GFP) under an autonomous CMV promoter—that is, cells that have taken up the shRNA vector are GFP-positive, which allows us to distinguish shRNA-transfected cells from non-transfected cells. We used Alexa Fluor 594–conjugated secondary antibody to label the SGLT1-IHC signal. The control shRNA transfected and non-transfected cells presented equal levels of SGLT1; however, the SGLT1 signal was significantly reduced in the SGLT1 shRNA–transfected cells compared with the control shRNA–transfected and non-transfected cells (Figure 2C). To further characterize SGLT1-IHC, we compared the immunohistochemical signals produced by SGLT1-IHC in the absence or presence of its blocking peptides in normal human intestine tissue, which is known to express SGLT1 [18] and a SGLT1 negative tissue, the brain [19]. SGLT1-IHC gave rise to clear positive signals in the epithelial cells of the small intestine, which were significantly reduced by its blocking peptides, and the brain tissue was completely

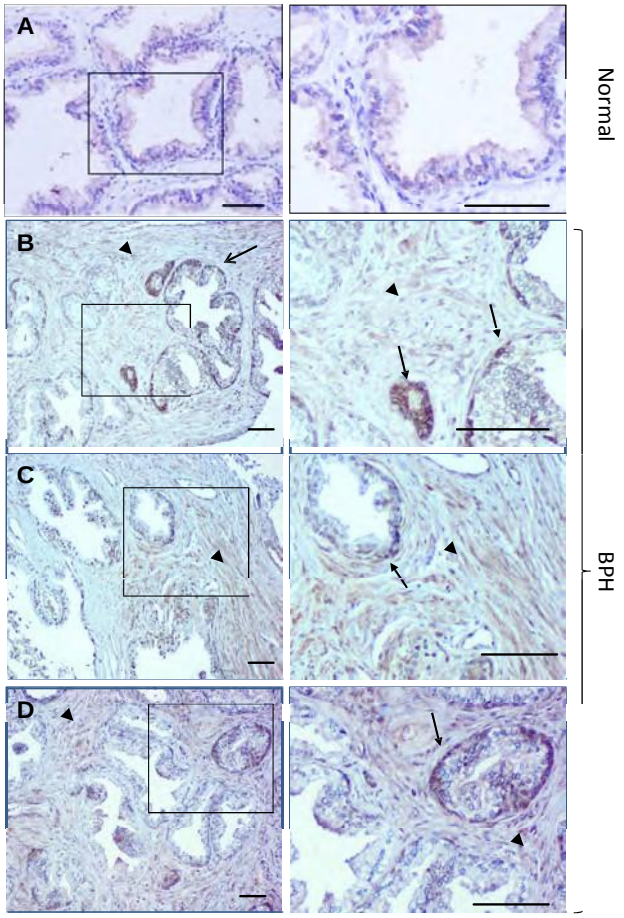

Figure 3: Expression of SGLT1 in normal and BPH prostate tissues. Immunohistochemical stained SGLT1-positive cells appear brown. Right panel is magnification of boxed area in left panel. **A**, Normal prostate. **B-D**, BPH tissues. Arrows point to basal cells, arrowheads indicate stromal cells. Bar=50 μm.

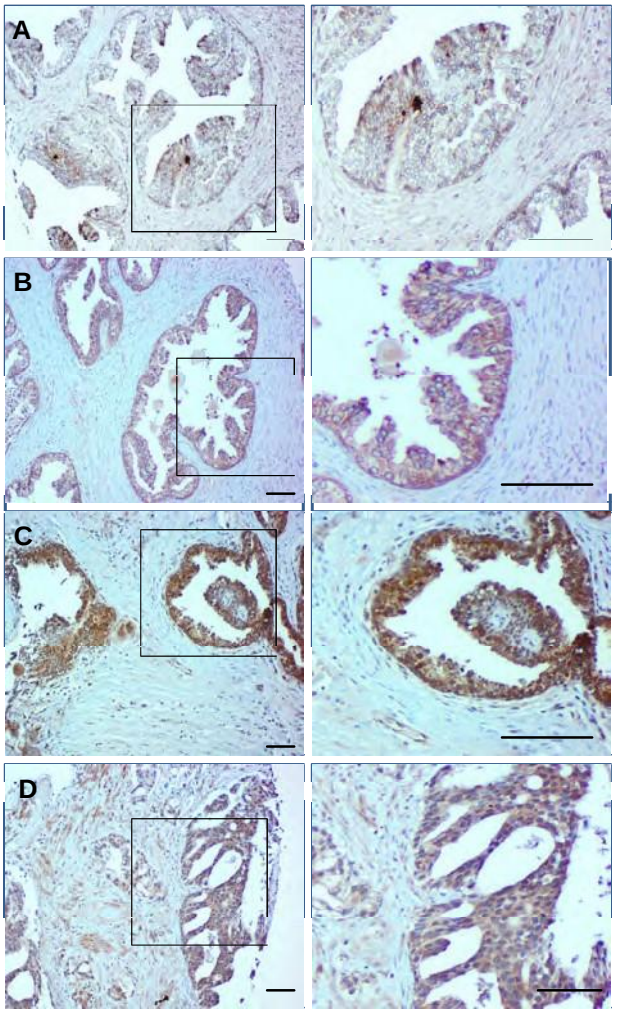

Figure 4: Expression of SGLT1 in PIN tissue. **A-D**, SGLT1-positive cells appear brown. Right panels are magnification of boxed areas in left panels. Bar=50 μm.

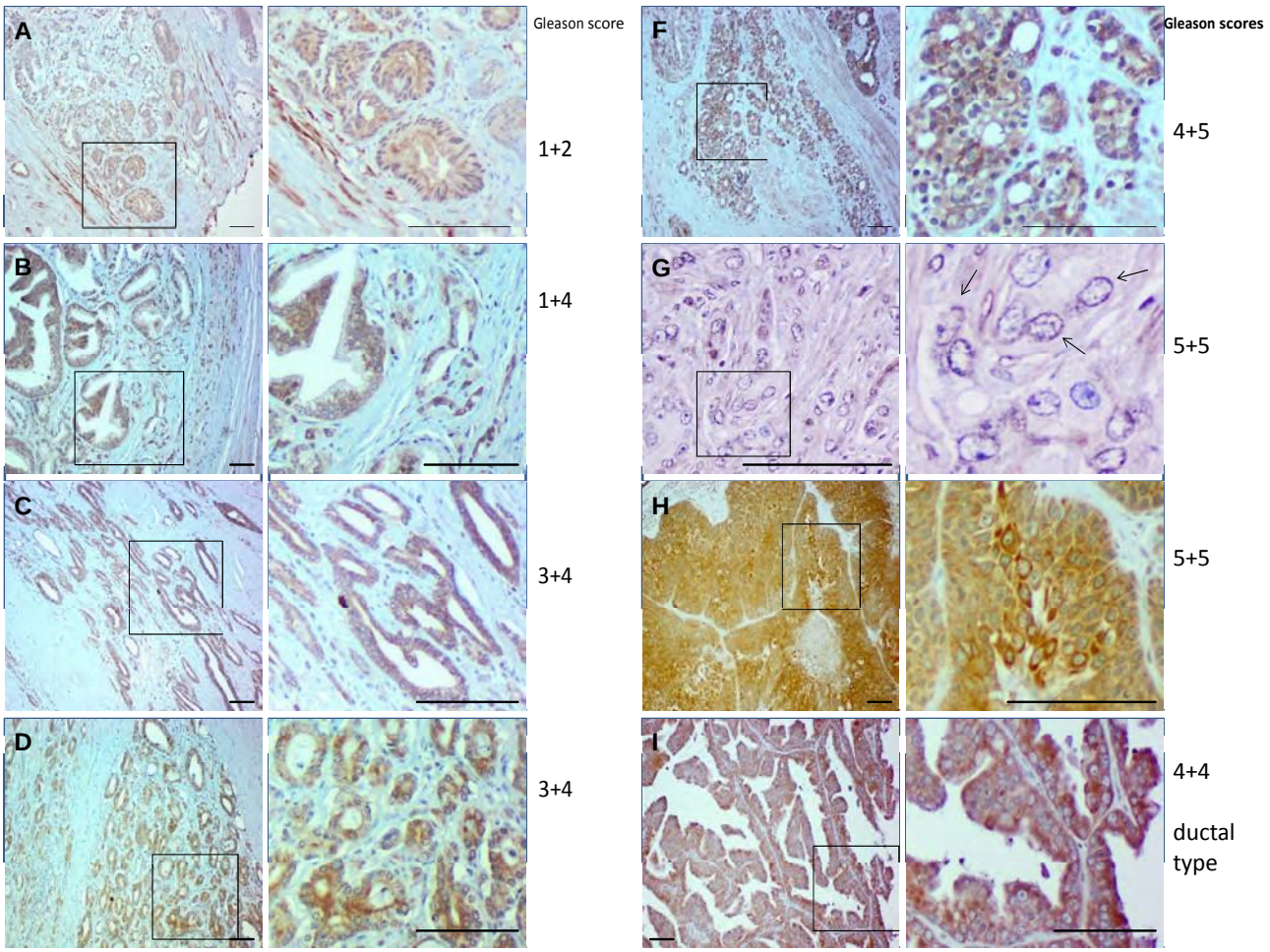

Figure 5: Expression of SGLT1 in PCa tissue representing different grades (Gleason scores). **A-I**, SGLT1-positive cells appear brown. Arrows in **G,** indicate SGLT1-positive nuclear envelopes. Right panels are magnification of boxed areas in left panels. Bar=50 μm.

negative (Figure 2D). Together, these results show that SGLT1-IHC is specific for endogenous SGLT1.

SGLT1 up-regulation in diseased human prostatic tissue: Using SGLT1-IHC, we profiled the expression of SGLT1 in samples of normal prostate (n=3), BPH (n=53), PIN (n=9), and PCa (n=44). SGLT1 was weakly expressed in the luminal epithelial cells of normal tissue (Figure 2D). All the BPH tissues had a discontinuous layer of basal cells with high levels of SGLT1 expression as well as SGLT1-positive stromal cells (Figure 3). Even greater SGLT1 expression was consistently observed in the epithelial cells of PIN samples (Figure 4). Cancer cells of all the prostate cancer samples were strongly positive for SGLT1 (Figure 5). Overall, the examples exhibited a pattern of membranous or cytoplasmic staining in cells of lower grade cancers and nuclear envelope staining in cells of high-grade cancers. SGLT1-positive stromal cells were also observed in PIN and PCa tissues but to a lesser extent than in the BPH samples. A semiquantitative summary of SGLT1 expression in these prostatic tissues is presented in Table 1.

SGLT1-positive, tenascin-negative stromal cells in diseased human prostatic tissue: Tissue stromal cells can be activated by pathological insults, which is often the case for diseased prostates [20,21]. Because we observed that stromal cells of BPH tissues and some PCa tissues were positive for SGLT1, we performed immunofluorescent co-staining of SGLT1 with a reactive stromal cell marker, tenascin [21], to determine whether the SGLT1-positive stromal cells were reactive stromal cells. To our surprise, the SGLT1-positive stromal cells were tenascin negative (Figure 6), suggesting they are not reactive stromal cells in BPH or PCa tissue.

Discussion

The normal human prostate gland produces, accumulates, and secrets high levels of citrate, which is predominantly derived from the oxidation of fatty acids [22]. Because the normal prostate is not active in glucose metabolism but relies on fatty acid metabolism, the role of glucose and its transporters in prostate biology has not been adequately investigated. However, emerging data suggest that both BPH and PCa are associated with altered glucose metabolism. Blood glucose levels positively correlate with prostate size in BPH [23] and the incidence of both BPH and PCa correlates with metabolic syndrome [24] of which glucose intolerance is one of the major abnormalities. In addition, high-grade PCa and PCa metastases exhibit increased glucose uptake [15,25]. Moreover, PCa cells are sensitive to glucose starvation–

induced autophagy [26]. The cumulative evidence strongly suggests that glucose metabolism is critically involved in the pathogenesis of prostate diseases, such as BPH and PCa.

Our study shows that the expression of SGLT1 is significantly increased in basal cells and stromal cells of BPH tissue compared with normal prostate tissue. The heterogeneous expression of SGLT1 in the basal cells and stromal cells of BPH is intriguing, which suggests that neither cell type is metabolically homogenous. These results strongly suggest a one-way glucose flux from the basal cells to the luminal epithelial cells in the normal prostate. The biological roles of SGLT1-positive basal cells and stromal cells in the pathogenesis of BPH demand further study.

The highly increased expression of SGLT1 in the epithelial cells of PIN and PCa cells relative to the cells of normal prostate and BPH tissues suggests that a high level of glucose is required during the pathogenesis of PCa. GLUT1 has been found to be expressed exclusively in luminal epithelial cells and in borders between the basal and luminal epithelial cells [17] and GLUT1 expression is decreased in PCa cells compared with non-cancer cells [16,17]. This shift from GLUT1 to SGLT1 in epithelial cells indicates a higher demand for glucose during the pathogenesis of PCa.

The stroma of PCa tissues also contains regions with a variable amount of SGLT1-positive stromal cells; these cells are not tenascin-positive reactive stromal cells [27]. Reactive stromal cells have been show to play critical roles in the pathogenesis of BPH and PCa [20,28]. These data added another layer of complexity to our increasing understanding of the role of stromal cells in the development of PCa and BPH. The variability of SGLT1-positive stroma in PCa might contribute to the lack of consistency between ^{18}F-fluoro-2-deoxy-2-D-glucose (FDG) positron emission tomography results of early-stage PCa [29] when tumor foci are small and scattered, because the FDG uptake by SGLT1-positive stromal cells may overshadow the uptake by cancer foci. The translocation of SGLT1 into the nuclear envelope of high-grade PCa that we observed is also intriguing and is reminiscent of proteins such as pyruvate kinase M2 [30] protein kinase C η [31] CXCR4 [32] annexin A1 [33] and EGFR [34] that reside in the non-nuclear compartments of normal cells and translocate to the nucleus of cancer cells, where they are involved in nuclear events critical for cancer cell proliferation and survival.

Tissue	No. of samples	Cell type		
		Luminal epithelial	Basal	SGLT1-postive stromal cells (%) **
Normal	3	+	+	Stromal cells are negative
BPH	53	+ and -	+++	62.4 ± 31.7
PIN	9	++	++	NA
PCa	44	+++	NA	++ to +++, 3.8 ± 5.4%

*The semi-quantification was carried out by two individuals in a blinded manner using the same normal prostate tissue as a standard reference. The signal density of normal prostate epithelial cells is considered as "+", and the signal density of the basal cells of BPH is considered as "+++".
**SGLT1-positive cells and total stromal cells were counted from 3 random selected areas under 200x magnification, and the percentage of SGLT1-positive cells is calculated by the number of SGLT1-positive cells/total stromal cells. The values are presented as mean ± SD.
NA: not applicable

Table 1: Expression level of SGLT1 in prostate tissue by cell type*.

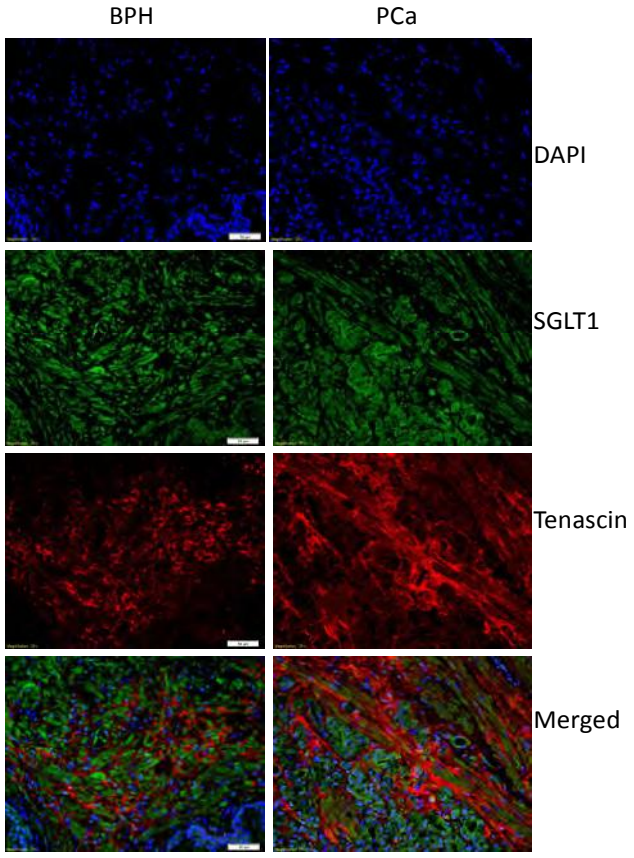

Figure 6: SGLT1-positive stromal cells are negative for tenascin. Immunofluorescent co-staining of SGLT1 (green) and tenascin (red) on tissue samples of BPH (**left**) and PCa (**right**). Nuclei were stained by DAPI (blue). Co-expression of SGLT1 and tenascin would have appeared yellow. Bar=50 μm.

The overall expression pattern of SGLT1 in normal prostate, BPH, and PCa tissues is very similar to the expression pattern of EGFR, which is weakly expressed in the epithelial cells of normal prostate tissue, moderately expressed in the stromal cells in BPH, and significantly increased in cancer cells [35-38]. These findings suggest that SGLT1 and EGFR expression might be regulated under a common mechanism, and they support our previous finding that EGFR interacts with or stabilizes SGLT1 in PCa cells [39]. Further investigation is needed to understand the association between EGFR and SGLT1 during the development of PCa.

Acknowledgement

This study is supported in part by grants from American Cancer Society and Department of Defense Prostate Cancer Research Program to Z. W.

References

1. Zhao FQ, Keating AF (2007) Functional properties and genomics of glucose transporters. Curr Genomics 8: 113-128.
2. Wright EM, Loo DD, Hirayama BA (2011) Biology of human sodium glucose transporters. Physiol Rev 91: 733-794.
3. Castaneda-Sceppa C, Castaneda F (2011) Sodium-dependent glucose transporter protein as a potential therapeutic target for improving glycemic control in diabetes. Nutr Rev 69: 720-729.
4. Diez-Sampedro A, Hirayama BA, Osswald C, Gorboulev V, Baumgarten K, et al. (2003) A glucose sensor hiding in a family of transporters. Proc Natl Acad Sci U S A 100: 11753-11758.

5. Vannucci SJ, Seaman LB, Vannucci RC (1996) Effects of hypoxia-ischemia on GLUT1 and GLUT3 glucose transporters in immature rat brain. J Cereb Blood Flow Metab 16: 77-81.

6. Peansukmanee S, Vaughan-Thomas A, Carter SD, Clegg PD, Taylor S, et al. (2009) Effects of hypoxia on glucose transport in primary equine chondrocytes *in vitro* and evidence of reduced GLUT1 gene expression in pathologic cartilage *in vivo*. J Orthop Res 27: 529-535.

7. Gamelli RL, Liu H, He LK, Hofmann CA (1996) Augmentations of glucose uptake and glucose transporter-1 in macrophages following thermal injury and sepsis in mice. J Leukoc Biol 59: 639-647.

8. Mann GE, Yudilevich DL, Sobrevia L (2003) Regulation of amino acid and glucose transporters in endothelial and smooth muscle cells. Physiol Rev 83: 183-252.

9. Macheda ML, Rogers S, Best JD (2005) Molecular and cellular regulation of glucose transporter (GLUT) proteins in cancer. J Cell Physiol 202: 654-662.

10. Hanabata Y, Nakajima Y, Morita K, Kayamori K, Omura K (2012) Coexpression of SGLT1 and EGFR is associated with tumor differentiation in oral squamous cell carcinoma. Odontology 100: 156-163.

11. Guo GF, Cai YC, Zhang B, Xu RH, Qiu HJ, et al. Overexpression of SGLT1 and EGFR in colorectal cancer showing a correlation with the prognosis. Med Oncol 28: S197-S203.

12. Casneuf VF, Fonteyne P, Van Damme N, Demetter P, Pauwels P, et al. (2008) Expression of SGLT1, Bcl-2 and p53 in primary pancreatic cancer related to survival. Cancer Invest 26: 852-859.

13. Lai B, Xiao Y, Pu H, Cao Q, Jing H, et al. (2012) Overexpression of SGLT1 is correlated with tumor development and poor prognosis of ovarian carcinoma. Arch Gynecol Obstet 285: 1455-1461.

14. Costello LC, Franklin RB (2000) The intermediary metabolism of the prostate: a key to understanding the pathogenesis and progression of prostate malignancy. Oncology 59: 269-282.

15. Shiiba M, Ishihara K, Kimura G, Kuwako T, Yoshihara H, et al. (2011) Evaluation of primary prostate cancer using 11C-methionine-PET/CT and 18F-FDG-PET/CT. Ann Nucl Med 26: 138-145.

16. Godoy A, Ulloa V, Rodríguez F, Reinicke K, Yañez AJ, et al. (2006) Differential subcellular distribution of glucose transporters GLUT1-6 and GLUT9 in human cancer: ultrastructural localization of GLUT1 and GLUT5 in breast tumor tissues. J Cell Physiol 207: 614-627.

17. Reinicke K, Sotomayor P, Cisterna P, Delgado C, Nualart F, et al. (2011) Cellular distribution of Glut-1 and Glut-5 in benign and malignant human prostate tissue. J Cell Biochem 113: 553-562.

18. Gorboulev V, Schürmann A, Vallon V, Kipp H, Jaschke A, et al. (2012) Na(+)-D-glucose cotransporter SGLT1 is pivotal for intestinal glucose absorption and glucose-dependent incretin secretion. Diabetes 61: 187-196.

19. Lee WS, Kanai Y, Wells RG, Hediger MA (1994) The high affinity Na+/glucose cotransporter. Re-evaluation of function and distribution of expression. J Biol Chem 269: 12032-12039.

20. Schauer IG, Rowley DR (2011) The functional role of reactive stroma in benign prostatic hyperplasia. 82: 200-210.

21. Tuxhorn JA, Ayala GE, Rowley DR (2001) Reactive stroma in prostate cancer progression. J Urol 166: 2472-2483.

22. Liu Y (2006) Fatty acid oxidation is a dominant bioenergetic pathway in prostate cancer. Prostate Cancer Prostatic Dis 9: 230-234.

23. Kim WT, Yun SJ, Choi YD, Kim GY, Moon SK, et al. (2011) Prostate size correlates with fasting blood glucose in non-diabetic benign prostatic hyperplasia patients with normal testosterone levels. J Korean Med Sci 26: 1214-1218.

24. Kasturi S, Russell S, McVary KT (2006) Metabolic syndrome and lower urinary tract symptoms secondary to benign prostatic hyperplasia. Curr Urol Rep 7: 288-292.

25. Schöder H, Larson SM (2004) Positron emission tomography for prostate, bladder, and renal cancer. Semin Nucl Med 34: 274-292.

26. DiPaola RS, Dvorzhinski D, Thalasila A, Garikapaty V, Doram D, et al. (2008) Therapeutic starvation and autophagy in prostate cancer: a new paradigm for targeting metabolism in cancer therapy. Prostate 68: 1743-1752.

27. Ayala G, Tuxhorn JA, Wheeler TM, Frolov A, Scardino PT, et al. (2003) Reactive stroma as a predictor of biochemical-free recurrence in prostate cancer. Clin Cancer Res 9: 4792-4801.

28. Tuxhorn JA, Ayala GE, Smith MJ, Smith VC, Dang TD, et al. (2002) Reactive stroma in human prostate cancer: induction of myofibroblast phenotype and extracellular matrix remodeling. Clin Cancer Res 8: 2912-2923.

29. Avril N, Dambha F, Murray I, Shamash J, Powles T, et al. (2010) The clinical advances of fluorine-2-D-deoxyglucose--positron emission tomography/computed tomography in urological cancers. Int J Urol 17: 501-511.

30. Yang W, Xia Y, Ji H, Zheng Y, Liang J, et al. (2011) Nuclear PKM2 regulates β-catenin transactivation upon EGFR activation. Nature 480:118-122.

31. Maissel A, Marom M, Shtutman M, Shahaf G, Livneh E (2006) PKCeta is localized in the Golgi, ER and nuclear envelope and translocates to the nuclear envelope upon PMA activation and serum-starvation: C1b domain and the pseudosubstrate containing fragment target PKCeta to the Golgi and the nuclear envelope. Cell Signal 18:1127-1139.

32. Wang SC, Lin JK, Wang HS, Yang SH, Li AF (2010) Nuclear expression of CXCR4 is associated with advanced colorectal cancer. Int J Colorectal Dis 25: 1185-1191.

33. Lin CY, Jeng YM, Chou HY, Hsu HC, Yuan RH, et al. (2008) Nuclear localization of annexin A1 is a prognostic factor in oral squamous cell carcinoma. J Surg Oncol 97: 544-550.

34. Li C, Iida M, Dunn EF, Ghia AJ, Wheeler DL (2009) Nuclear EGFR contributes to acquired resistance to cetuximab. Oncogene 28: 3801-3813.

35. Ibrahim GK, Kerns BJ, MacDonald JA, Ibrahim SN, Kinney RB, et al. (1993) Differential immunoreactivity of epidermal growth factor receptor in benign, dysplastic and malignant prostatic tissues. J Urol 149: 170-173.

36. De Miguel P, Royuela, Bethencourt R, Ruiz A, Fraile B, et al. (1999) Immunohistochemical comparative analysis of transforming growth factor alpha, epidermal growth factor, and epidermal growth factor receptor in normal, hyperplastic and neoplastic human prostates. Cytokine 11: 722-727.

37. Leav I, McNeal JE, Ziar J, Alroy J (1998) The localization of transforming growth factor alpha and epidermal growth factor receptor in stromal and epithelial compartments of developing human prostate and hyperplastic, dysplastic, and carcinomatous lesions. Hum Pathol 29: 668-675.

38. Sherwood ER, Lee C (1995) Epidermal growth factor-related peptides and the epidermal growth factor receptor in normal and malignant prostate. World J Urol 13: 290-296.

39. Weihua Z, Tsan R, Huang WC, Wu Q, Chiu CH, et al. (2008) Survival of cancer cells is maintained by EGFR independent of its kinase activity. Cancer Cell 13: 385-393.

The Prostate 71:1216^1224 (2011)

Loss of EGFR Induced Autophagy Sensitizes Hormone Refractory Prostate Cancer Cells to Adriamycin

Shuping Xu[1] and Zhang Weihua[2]*

[1]Department of Urology, University of Pittsburgh Cancer Center, University of Pittsburgh, Pittsburgh, Pennsylvania
[2]Center for Nuclear Receptors and Cell Signaling, Department of Biochemistry and Biology, College of Natural Science and Mathematics, University of Houston, Houston, Texas

BACKGROUND. The epidermal growth factor receptor (EGFR), a receptor tyrosine kinase, is over-expressed in advanced prostate cancer but tyrosine kinase inhibitors are not clinically effective in the treatment of prostate cancer. Recently it was found that EGFR in cancer cells has a kinase-independent pro-survival function, preventing cells from undergoing autophagy. In the present study we investigated whether the anti-autophagic function of EGFR may contribute to resistance of hormone-refractory prostate cancer cells to chemotherapeutic-induced apoptosis.
METHODS. We first characterized the autophagic phenotype induced by knocking down EGFR in hormone refractory prostate cancer cells (PC-3MM2 and DU-145), then we tested whether loss of EGFR-induced autophagy could sensitize cancer cells to adriamycin.
RESULTS. Using continuous live cell imaging techniques, we observed that knocking down EGFR lead to typical autophagic morphological/molecular changes, cell shrinkage without detachment, aggregation of microtubule-associated protein 1 light chain 3 (LC3) protein and absence of activation of apoptotic caspases 3/7. Loss of EGFR also increased the activity of calpain, which is pro-apoptotic. Knocking down EGFR, but not inhibiting its tyrosine kinase activity, significantly sensitized cells to adriamycin-induced apoptosis. Adriamycin-induced apoptosis could be inhibited by increased extracellular glucose level, suggesting intracellular glucose deficiency is a key mediator of the sensitization. The loss of EGFR induced autophagy and sensitization to adriamycin were also reproduced by using another hormone refractory prostate cancer cell line, Du145.
CONCLUSION. Taken together, these data suggest that decreasing the expression level of EGFR protein, rather than inhibiting its tyrosine kinase activity, may enhance the efficiency of EGFR targeted therapy for prostate cancer. Prostate 71: 1216–1224, 2011.
Published 2011 Wiley-Liss, Inc.[y]

KEY WORDS: EGFR; kinase independent function; prostate cancer; autophagy; drug resistance

INTRODUCTION

The epidermal growth factor receptor (EGFR) is over-active in most types of tumors of epithelial origin [1]. Since EGFR is a receptor tyrosine kinase and activation of EGFR most often results in cell proliferation and enhanced cell survival, blocking the tyrosine kinase activity of EGFR has been a strategy of cancer therapy. Analogues of ATP that can compete for binding of ATP to EGFR in either competitive or non-competitive manners have been developed, and some have already been used in the clinic [2].

In prostate cancer, EGFR is elevated along with disease progression. In the normal prostate EGFR expression is low [3]. Compared to the tumor cells of the primary site, it was found that prostate cancer bone metastases express significantly higher level of EGFR [4]. Studies have shown that increased levels of EGFR immunoreactivity in hormone-independent human prostate cancer cell lines [5,6]. More interestingly, EGFR expression increases as prostate cancer progresses from an androgen dependent to an androgen independent stage [7]. In tissues of patients with meta-

*Correspondence to: Zhang Weihua, 3605 Cullen Blvd, Houston, TX 77204-5056. E-mail: wzhang13@uh.edu
Received 23 September 2010; Accepted 9 December 2010
DOI 10.1002/pros.21337
Published online 12 January 2011 in Wiley Online Library (wileyonlinelibrary.com).

static androgen-independent prostate cancer, EGFR over-expression was detected in most cancer cells [8,9]. However, despite the positive correlation of the expression level of EGFR with disease progression, targeting EGFR kinase activity has not yet produced positive clinical outcomes for prostate cancer treatment [10].

Evidence supporting a kinase independent prosurvival function of EGFR exists. For example, both the wild-type and kinase-dead EGFR showed a pro-survival role in EGFR negative 32D hematopoietic cells [11]; knocking down EGFR with small interfering RNA (siRNA) resulted in cell death [12–14], while most often EGFR tyrosine kinase inhibitors cause cell growth arrest rather than cell death [15]; EGFR knockout animals die soon after birth [16], but animals with severely compromised EGFR kinase activity are completely viable and display only epithelial defects [17]. We have recently found that EGFR, independent of its kinase activity, protects cancer cells from undergoing autophagy [18].

Autophagy, a process of self-digestion providing cells with enough nutrients and energy substrates for survival [19], plays multi-faceted roles in tumor formation, progression, and drug resistance. The autophagy pathway can act as a tumor suppressor, a tumor protector, an anticancer drug-sensitizer or a desensitizer, depending on tumor type, stage and the kind of anticancer stimulus. Autophagy is tumor suppressive since mice that are haplo-insufficient for beclin 1, an upstream regulator of the autophagy pathway, are tumor-prone [20]. Loss of at least one allele of beclin 1, a protein required for autophagy, is found in many types of cancer cells [21]. Autophagy is also tumor protective since it enhances the survival of tumor cells in a nutrient deprived and hypoxic environment [22], which is a hallmark of solid tumors. Blocking the autophagy pathway sensitizes chronic myelogenous leukemia cells to an anticancer drug suberoylanilide hydroxamic acid (a histone deacetylase inhibitor) [23], while induction of autophagy sensitizes glioblastoma cells to chemotherapeutic agents [24].

To further explore the possibility of targeting EGFR for prostate cancer therapy, we investigated whether loss of EGFR-induced autophagy can affect the sensitivity of prostate cancer cells to the chemotherapeutic agent, adriamycin.

MATERIALS AND METHODS

Reagents

The human hormone refractory metastatic prostate cancer cell line PC-3MM2 selected from the parental PC3 line [25] was a gift from Dr. Isaiah Fidler (MD Anderson Cancer Center, Houston). Du145 prostate cancer cells were purchased from American Type of Cell Culture (Manassas, VA). Minimum essential medium (MEM) containing 5.5 mM glucose, fluorescent conjugated caspases 3/7 substrates was purchased from Invitrogen (San Diego, CA). Glucose was from Sigma–Aldrich (St. Louis, MO). Antibodies against EGFR and pEGFR were from Cell Signaling (Danvers, MA). Horse radish peroxidase conjugated secondary antibodies against mouse or rabbit and AG1478 were from Santa Cruz Biotech (Santa Cruz, CA). A calpain activity measurement kit was from Promega (Madison, WI). The U6 promoter-driven siRNA vector (pRNAT-U6.1/Neo for EGFR, SGLT1, and their scrambled controls) was constructed by Genscript Corp. (Piscataway, NJ). The target sequence for EGFR siRNA is CGCAAAGTGTGTAACGGAATA. The negative control siRNA sequence is GAACAATGTTGACCAGGTGA.

Cell Culture and Treatment

PC-3MM2 or DU145 cells were incubated in a high glucose (25 mM) containing MEM supplemented with 10% fetal bovine serum, sodium pyruvate, nonessential amino acids, L-glutamine in 5% CO_2-95% air at 378C. When cells were grown to about 70% confluence, cells were then either transfected with vectors expressing either control or EGFR siRNA using a transfection reagent, GeneJuice (EMD Chemicals, Gibbstown, NJ). At 48 hr after transfection, cell culture medium was replaced with high glucose medium containing 2 mg/ml G418 for selection of stable clones. After 3 weeks of selection, siRNA-expressing stable clones were pooled and the expression level of EGFR in control and EGFR siRNA knock down cells were measured using Western blotting analysis. To test the sensitivity of cells to adriamycin, triplicate samples of control and EGFR siRNA treated cells were seeded in six-well culture plates and cultured in high glucose MEM for 24 hr. Then the high glucose medium was replaced with medium containing 5 mM glucose, and cultured for 6 hr before drug treatment. There were five experimental groups for control cells: vehicle, AG1478 (500 nM), adriamycin (100 ng/ml), adriamycin/AG1478 and adriamycin/glucose (25 mM); there were six groups for EGFR siRNA treated cells: vehicle, AG1478, adriamycin, adriamycin/AG1478 and adriamycin/glucose (25 mM). At 24 hr after treatment, cells were harvested, fixed, and stained with propedium iodine for flow cytometry analysis.

Live Cell Imaging of Autophagy and the Activities of Caspases 3 and 7

A live cell monitoring system, Biostation (Nikon, NY), was used to produce continuous images of live

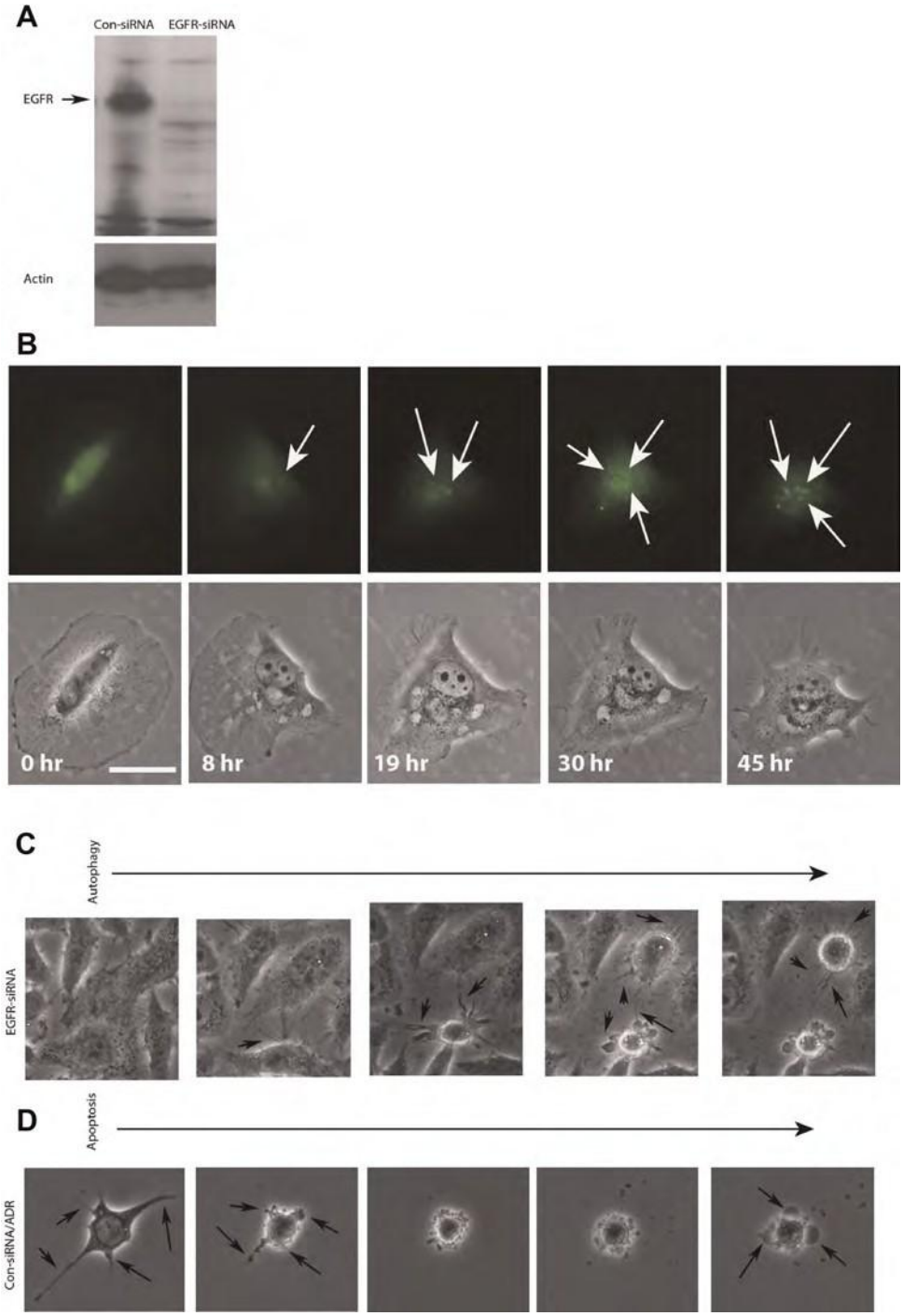

Fig. 1. Characterization of loss of EGFR induced autophay of PC3 -MM2 cells. A: Western Blotting analysis of EGFR expression after knocking down by siRNA. Beta-actin was used as the loading control (con-siRNA, cells stably transfected with control siRNA; EGFR-siRNA, cells stably transfected with siRNA against EGFR.) B: Time lapse imaging of formation of GFP-LC3 aggregates (arrows). Phase-contrast images were taken concurrently (bar ¼ 15 mm). C: Phase-contrast imaging of morphological changes of cells undergoing autophagic cell death induced by EGFR knockdown. Note cell shrinkage (arrow heads) without filopodia detachment (arrows). D: Phase-contrast imaging of morphological changes of cells undergoing apoptotic cell death induced by adriamycin (100 ng/ml). Note filopodia detachment (arrows) before cell shrinkage and membrane blebbing (arrows on the last image).

cells. To facilitate monitoring morphological changes and activation of caspases along with the process of autophagy, we transfected a GFP fused autophagic marker gene, microtubule-associated protein 1 light chain 3 (LC3) [26] into the control and EGFR siRNA cells. The GFP-LC3 positive cells were sorted out using a cell-sorter (BD FACSVantage SE system; BD Biosciences, Palo Alto, CA) that used green fluorescence as a selector. After cell sorting, GFP-LC3 positive cells were cultured in 35 mm cell culture dishes containing high glucose MEM. When cells completely attached, red fluorescent conjugated substrate of caspases 3/7, Image-iTLive (Invitrogen) was added into the culture medium at a final concentration of 30× dilution. After 10 min incubation, cells were washed with MEM containing 5 mM glucose and cultured in 5 mM glucose medium in the Biostation culture chamber and imaged at 5 min intervals with triple light sources for normal phase contrast, green fluorescent images (for GFP-LC3) and red fluorescent images (for monitoring the activities of caspases 3 and 7).

Western Blotting Analysis

Western blotting was used to determine the effects of EGFR siRNA on the expression level of EGFR, the level of activated EGFR (phosphorylated EGFR, pEGFR). In brief, cells were incubated for 10 min at 08C in a lysis buffer (50 mM HEPES, pH 7.4; 150 mM NaCl; 1.0% Triton X-100; 1.5 mM $MgCl_2$; 1 mM EDTA; and 1 mM phenylmethlysulfonyl fluoride). Equal amounts of proteins pooled from triplicate samples separated by 7% sodium dodecyl sulfate–polyacrylamide gel electrophoresis (SDS–PAGE) were transblotted to nitrocellulose, blocked with 5% nonfat dry milk for 2 hr at room temperature, and then incubated overnight with primary antibodies (rabbit anti-EGFR, rabbit anti-pEGFR, and rabbit anti-actin) (all at a 1:1,000 dilution). The primary antibody-bound membranes were washed for 10 min with a washing buffer (PBS solution containing 0.1% NP40) before incubation with corresponding secondary antibodies conjugated with horseradish peroxidase (all at a 1:3,000 dilution). After a 30-min washing, immunoreactive signals were visualized by enhanced chemiluminescence.

Measurement of Calpain Activity

Triplicate control and EGFR siRNA cells were cultured in high glucose MEM in a 96-well culture plate. When cells were grown to about 80% confluence, culture medium was replaced with MEM containing 5 mM glucose. At 24 hr after culturing in 5 mM glucose medium, cells were washed with calcium free PBS before calpain measurement. A kit for measurement of calpain activity was purchased from Promega. Calpain activity was measured according to protocols provided by the manufacturer.

Statistic Analysis

Student t-test was used to assess the difference of control and treated groups. $P < 0.05$ was defined as statistically significant.

RESULTS Characterization of Autophagic Cell Death Using Live Imaging

Previously, we found that knocking down EGFR in cancer cells resulted in autophagy, which is characterized by the appearance of autophagosomes [18]. To test the impact of loss of EGFR-induced autophagy on the sensitivity of cancer cells to adriamycin, we first had to establish a window in time when autophagy is taking place. To this end, we performed a live imaging characterization of the autophagy induced by knocking down EGFR. Since EGFR knocked down cells do not undergo autophagy when cultured in medium containing high level of glucose (25 mM) [18], for the purpose of live imaging autophagy, we were able to transfect green fluorescent protein conjugated microtubule-associated protein 1 light chain 3 (GFP-LC3) [26] into EGFR knocked down cells cultured in high glucose medium. Formation of aggregates of GFP-LC3 was used as an indicator of autophagy. Positive cells were sorted out using GFP as an indicator. To measure apoptosis in parallel, the GFP-LC3 labeled EGFR siRNA and control siRNA cells were then incubated with a red fluorescent indicator of caspases 3/7. Continuous live imaging of cell morphology, motion of GFP-LC3 and activity of caspase 3/7 was carried out by Biostation live imaging system concurrently. As shown in Figure 1A, measured

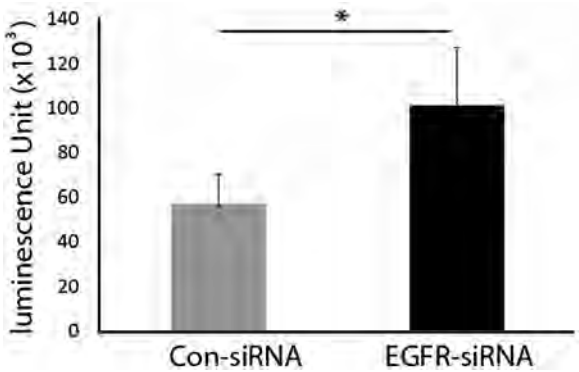

Fig. 2. Measurement of calpain activity of PC3-MM2 cells. The activity of calpain in control-siRNA and EGFR-siRNA cells was measured at the 36 hr time point of cells cultured in medium containing 5.5 mM glucose (samples in triplicates were used in each group, $^{*}P < 0.05$).

by Western blotting, the pool of cells transfected with EGFR siRNA has a significantly lower EGFR level than the pool of cells transfected with control siRNA. The formation of GFP-LC3 aggregates occurred between 8 and 48 hr after cells were cultured in medium containing 5.5 mM glucose (Fig. 1B). The morphological changes during autophagic cell death were monitored in comparison with adriamycin induced apoptotic cell death. As shown in Figure 1C, EGFR knockdown of induced cell death characterized by two major morphological changes: (1) cell body shrinkage and (2) lack of detachment from the culture dish. The adriamycin-induced cell death presented typical features of apoptotic cell death: detachment, cell body shrinkage, and membrane blebbing (Fig. 1D).

Since calpain is involved in connecting autophagy with apoptosis [27] and our goal was to test whether loss of EGFR-induced autophagy could sensitize hormone refractory prostate cancer cells to the apoptotic toxicity of adriamycin, we measured the activity of calpain in cells carrying EGFR siRNA and in control cells cultured in medium containing 5.5 mM glucose for 24 hr. As shown in Figure 2, the calpain activity of EGFR siRNA-treated cells was significantly higher than that of the control cells, indicating that knocking down EGFR predisposed cells to apoptosis.

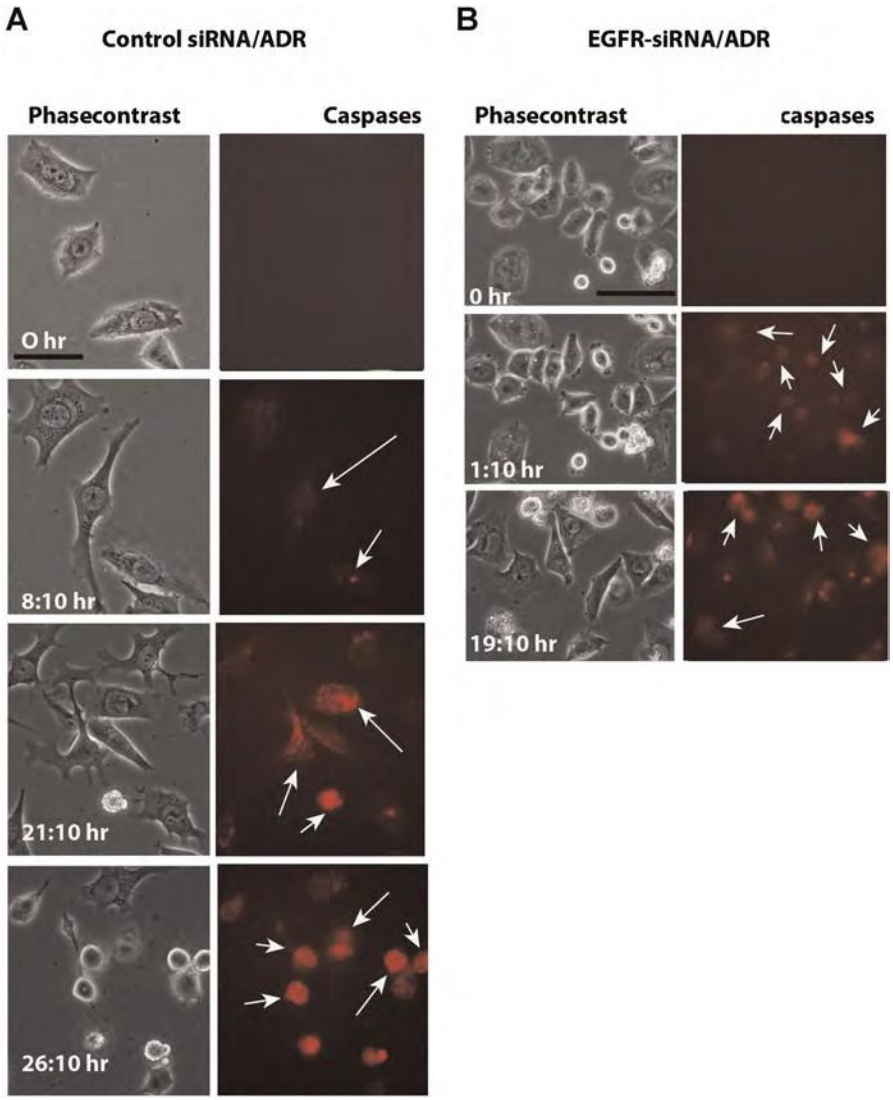

Fig. 3. Live imaging of activation of caspases 3/7 of PC3-MM2 cells treated with adriamycin. A: Control-siRNA cells were pre-incubated with Image-iTLive Red fluorescent substrates of caspases 3/7 for 10 min, then treated with adriamycin (100 ng/ml). Time-lapse images were taken. Activated caspases 3/7 appeared at about 8 hr after adriamycin treatment (arrows) and lasted till about 26 hr when the majority of cells were apoptotic. B: EGFR-siRNA cells were pre-incubated with Image-iTLive Red fluorescent substrates of caspases 3/7 for 10 min, then treated with adriamycin (100 ng/ml). Time-lapse images were taken. Activated caspases 3/7 appeared at about 1 hr after adriamycin treatment (arrows) and lasted till about 19 hr when the majority of cells were apoptotic (bar ¼ 50 mm).

Knocking Down EGFR, But Not Inhibiting its Tyrosine Kinase Activity, Sensitized Prostate Cancer Cells to Adriamycin-Induced, Glucose Sensitive Autophagy

Knowing the window of autophagy induced by knockdown of EGFR of PC3-MM2 is between 8 and 48 hr after culturing in medium containing 5.5 mM glucose, we then tested whether the effect of knocking down EGFR on the sensitivity of hormone refractory prostate cancer cells to a common chemotherapeutic drug, adriamycin. Using dual-color live imaging, red fluorescence for caspases 3/7 and green fluorescence for GFP-LC3, the processes of autophagy and apoptosis of live cells were monitored concurrently. As shown in Figure 3A, AG1478 efficiently inhibited the phosphorylation of EGFR of cells treated with AG1478 alone or cells treated with AG1478 combined with adriamycin. When the activity of caspases 3/7 were imaged, it was found that adriamycin caused activation of caspases 3/7 in cells with control siRNA at 8 hr; while EGFR siRNA cells were sensitive to adriamycin with caspases 3/7 being activated at 1 hr after treatment (Fig. 3B). The treatment induced cell death was quantified using flow cytometry. As shown in Figure 4A, AG1478 showed efficient inhibitory effect on the phosphorylation of EGFR, but had no effect on the cytotoxicity of adriamycin (Fig. 4B); on the other hand, knocking down EGFR significantly enhanced the cytotoxicity of adriamycin. Since increases in extracellular glucose level can inhibit loss of EGFR-induced autophagy, we tested whether it could also inhibit the loss of EGFR-induced sensitization of cancer cells to adriamycin. Culturing cells in medium containing 25 mM glucose completely reversed the loss of EGFR-induced sensitization of PC3-MM2 cells to adriamycin (Fig. 4B).

To test whether loss of EGFR can also sensitize another type of commonly used hormone refractory prostate cancer cell to adriamycin, we knocked down EGFR of Du145 cells with siRNA. As shown in Figure 5A, the content of EGFR of Du145 cells was reduced by more than 70% by siRNA. Culturing cells in 5.5 mM glucose containing medium resulted in cleavage of LC3 of EGFR-siRNA treated cells at 36 hr, however, which could not be completely blocked by treating cells with 25 mM glucose (Fig. 5B). When these cells were treated with adriamycin in the presence/absence of AG1478, it was found that, similar to PC3-MM2 cells, loss of EGFR but not inhibiting its kinase activity significantly sensitized Du145 cells to adriamycin (Fig. 5C). The loss of EGFR induced sensitization to adriamycin; however, this sensitivity could not be inhibited by 25 mM glucose treatment (Fig. 5C).

DISCUSSION

Although EGFR is over-expressed in prostate cancers, especially cancers of advanced stages [8,9], disappointingly, no beneficial effect has been observed when targeting the kinase activity of EGFR is combined with standard chemotherapies [10,28–31]. Over-expression of EGFR contributes significantly to the progression of prostate cancer, particularly to the development of hormone-refractory phase [32–34]. The clinical failure of targeting the kinase of EGFR for prostate cancer treatment warrants a re-evaluation on the value of EGFR as a therapeutic target for this type of cancer.

We have recently reported that EGFR has a kinase independent pro-survival function, preventing cancer cells from undergoing autophagy by maintaining

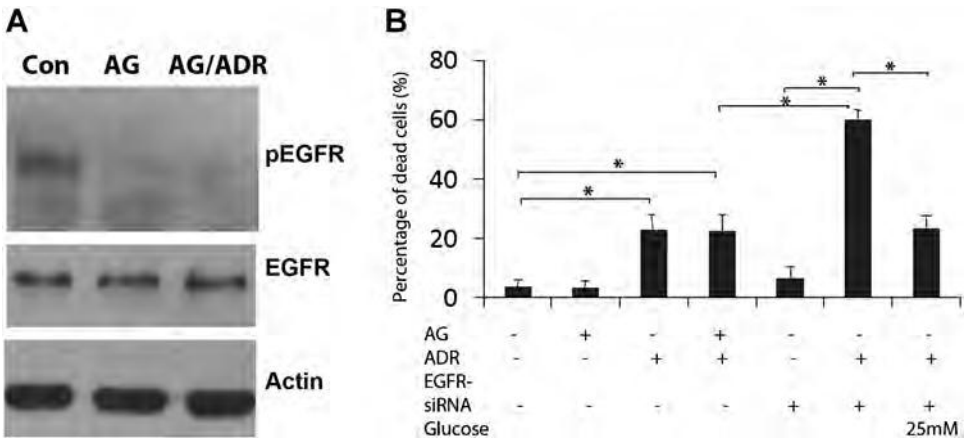

Fig. 4. Comparisons of cytotoxicity of adriamycin on PC3-MM2 cells treated with AG1478 and EGFR-siRNA. A: Western Blotting analysis of phosphorylated EGFR (pEGFR) of control (Con), AG1478 treated (AG) and AG1478 þ adriamycin (AG/ADR). Total EGFR (EGFR) and actin were used as loading controls. B: Flow cytometry measurement of sub-G1 cells. Samples were harvested at 24 hr after treatment (samples in triplicates were used in each group) (values ¼ mean ± SD, * statistic difference between linked groups, $P < 0.05$).

intracellular glucose [18]. The autophagic phenotype caused by knocking down EGFR was further characterized in this study. Evidence supporting a crucial kinase independent function of EGFR exists. EGFR knockout animals die soon after birth [16], but animals with severely compromised EGFR kinase activity are completely viable and display only epithelial defects [17]. In one study, both the wild-type and kinase-dead EGFR showed a pro-survival role in EGFR negative 32D hematopoietic cells [11].

Although EGFR contributes to cell survival, data supporting a role for EGFR tyrosine kinase activity in this cellular function remains inconclusive. Two types of cell survival exist: basal-survival and survival-under-stress. Basal-survival refers to cells maintaining a viable status under normal physiological conditions while survival-under-stress refers to the ability of cells to remain viable under harmful conditions, such as exposure to cytotoxic compounds, irradiation, hypoxia, etc. The molecular mechanisms underlying basic-survival and survival-under-stress may not necessarily coincide. Treating cells with EGFR tyrosine kinase inhibitors alone normally leads to cell growth arrest, not cell death [35,36], but co-treatment of cells with EGFR kinase inhibitors and cytotoxic stimuli, such as chemotherapeutic drugs, apoptotic inducers, and irradiation, results in enhanced cell death [5,37,38]. Overexpression of wild-type EGFR promotes cell survival in conditions of cytotoxic stress [39,40]. What is not easy to understand is why pre-treatment with EGFR tyrosine kinase inhibitors protects cells from chemotherapeutic drugs [41–43]. These conflicting data could be due to the timing of EGFR kinase inhibition. The synergistic cytotoxic effect produced by co-treatment of cells with EGFR tyrosine kinase inhibitors and cytotoxic drugs might be explained by the instant suppression of cell survival pathways, such as PI3-Akt and MAPK pathways, by tyrosine kinase inhibition [40]. On the other hand, pre-treatment of cells with tyrosine kinase inhibitors results in cell growth arrest at the G1 phase of cell cycle, and arrest at G1 promotes resistance to certain chemotherapeutic drugs [44,45].

The autophagic response caused by knocking down EGFR but not by inhibiting its kinase [12,13,18] suggests that EGFR has a kinase independent pro-basal-survival function and opens a new window of targeting EGFR for prostate cancer therapy. Autophagy can sensitize cells to apoptosis via activation of calpain [27], a calcium-dependent non-lysosomal cysteine protease. As predicated, treatment of EGFR knock-down cells with adriamycin at the window when autophagy is ongoing (within 45 hr after culturing in medium containing 5.5 mM glucose) caused significantly more apoptotic cell death than co-treating cells with EGFR

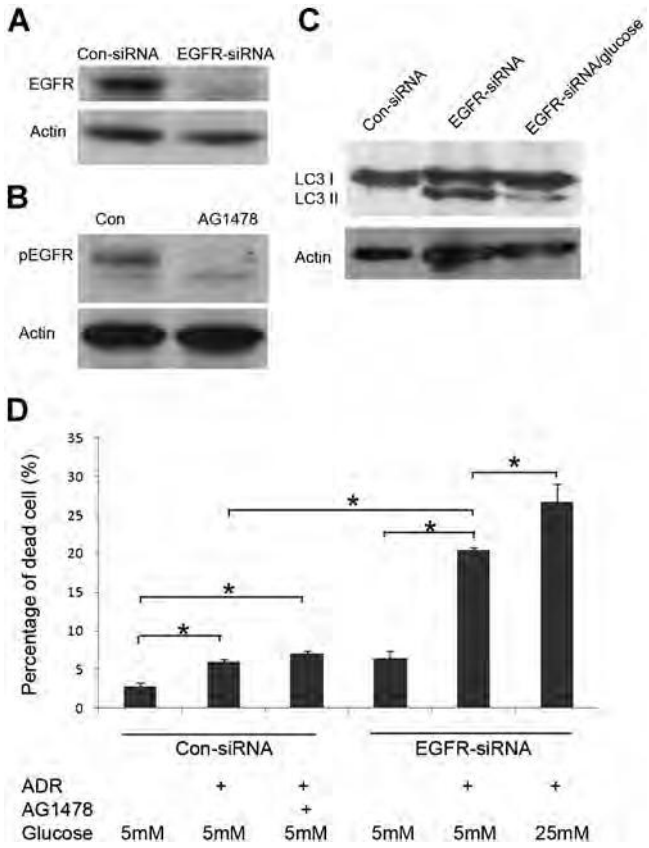

Fig. 5. Knocking down EGFR sensitized Du145 cells to adriamycin. A: Western blotting analysis of EGFR level of control-siRNA and EGFR-siRNA treated cells and effect of AG1478 on the phosphorylation of EGFR. B: Measurement of calpain activity of control-siRNA and EGFR-siRNA treated cells. C: Western blotting analysis of LC3 cleavage of EGFR-siRNA treated cells cultured in medium containing either 5.5 mM or 25 mM glucose. D: Flow cytometry measurement of sub-G1 cells. Samples were harvested at 36 hr after treatment (samples in triplicates were used in each group) (values ¼ mean ± SD, * statistic difference between linked groups, $P < 0.05$).

kinase inhibitor, AG1478, and adriamycin. The early death in EGFR knock-down cells correlated with a much earlier activation of caspases 3/7.

Previously we found that knockdown of EGFR induced autophagy was extracellular glucose dependent [18]. This also applies to the EGFR knockdown induced sensitization of PC3-MM2 cells to adriamycin, which was completely reversed by 25 mM glucose. Knocking down EGFR in another hormone refractory prostate cancer cell line, Du145, also resulted in sensitization to adriamycin. However, 25 mM glucose failed to rescue the EGFR knockdown induced sensitization of Du145 cells to adriamycin, which suggests that loss of EGFR induced autophagic phenotypes of PC3-MM2 and Du145 are mediated by different mechanisms. Prostate cancer cells differ in their metabolisms [46]

and expression of metabolic related genes such as p53 [47,48]. While the mechanism that prevents adriamycin treated Du145-EGFR knockdown cells from being rescued by glucose warrants further investigation, nevertheless, loss of EGFR lead to sensitization of both types of hormone refractory prostate cancer cells to adriamycin. It is concluded that decreasing the amount of EGFR protein might be an effective approach for EGFR targeted therapy for prostate cancer.

ACKNOWLEDGMENTS

This study was supported in part by American Cancer Society, by Department of Defense Prostate Cancer Research Program, the Center of Nuclear Receptor and Cell Signaling of University of Houston and the Department of Urology of University of Pittsburgh.

REFERENCES

1. Khalil MY, Grandis JR, Shin DM. Targeting epidermal growth factor receptor: Novel therapeutics in the management of cancer. Expert Rev Anticancer Ther 2003;3(3):367–380.
2. Herbst RS, Sandler AB. Overview of the current status of human epidermal growth factor receptor inhibitors in lung cancer. Clin Lung Cancer 2004;6 (Suppl 1):S7–S19.
3. Letellier G, Perez MJ, Yacoub M, Levillain P, Cussenot O, Fromont G. Epithelial phenotypes in the developing human prostate. J Histochem Cytochem 2007;55(9):885–890.
4. Zellweger T, Ninck C, Bloch M, Mirlacher M, Koivisto PA, Helin HJ, Mihatsch MJ, Gasser TC, Bubendorf L. Expression patterns of potential therapeutic targets in prostate cancer. Int J Cancer 2005;113(4):619–628.
5. Pu YS, Hsieh MW, Wang CW, Liu GY, Huang CY, Lin CC, Guan JY, Lin SR, Hour TC. Epidermal growth factor receptor inhibitor (PD168393) potentiates cytotoxic effects of paclitaxel against androgen-independent prostate cancer cells. Biochem Pharmacol 2006;71(6):751–760.
6. Sherwood ER, Lee C. Epidermal growth factor-related peptides and the epidermal growth factor receptor in normal and malignant prostate. World J Urol 1995;13(5):290–296.
7. Hernes E, Fossa SD, Berner A, Otnes B, Nesland JM. Expression of the epidermal growth factor receptor family in prostate carcinoma before and during androgen-independence. Br J Cancer 2004;90(2):449–454.
8. Di Lorenzo G, Tortora G, D'Armiento FP, De Rosa G, Staibano S, Autorino R, D'Armiento M, De Laurentiis M, De Placido S, Catalano G, Bianco AR, Ciardiello F. Expression of epidermal growth factor receptor correlates with disease relapse and progression to androgen-independence in human prostate cancer. Clin Cancer Res 2002;8(11):3438–3444.
9. Scher HI, Sarkis A, Reuter V, Cohen D, Netto G, Petrylak D, Lianes P, Fuks Z, Mendelsohn J, Cordon-Cardo C. Changing pattern of expression of the epidermal growth factor receptor and transforming growth factor alpha in the progression of prostatic neoplasms. Clin Cancer Res 1995;1(5):545–550.
10. Gross M, Higano C, Pantuck A, Castellanos O, Green E, Nguyen K, Agus DB. A phase II trial of docetaxel and erlotinib as first-line therapy for elderly patients with androgen-independent prostate cancer. BMC Cancer 2007;7:142.
11. Ewald JA, Wilkinson JC, Guyer CA, Staros JV. Ligand- and kinase activity-independent cell survival mediated by the epidermal growth factor receptor expressed in 32D cells. Exp Cell Res 2003;282(2):121–131.
12. Kang CS, Zhang ZY, Jia ZF, Wang GX, Qiu MZ, Zhou HX, Yu SZ, Chang J, Jiang H, Pu PY. Suppression of EGFR expression by antisense or small interference RNA inhibits U251 glioma cell growth in vitro and in vivo. Cancer Gene Ther 2006;13(5):530–538.
13. Nagy P, Arndt-Jovin DJ, Jovin TM. Small interfering RNAs suppress the expression of endogenous and GFP-fused epidermal growth factor receptor (erbB1) and induce apoptosis in erbB1-overexpressing cells. Exp Cell Res 2003;285(1):39–49.
14. Wu X, Deng Y, Wang G, Tao K. Combining siRNAs at two different sites in the EGFR to suppress its expression, induce apoptosis, and enhance 5-fluorouracil sensitivity of colon cancer cells. J Surg Res 2007;138(1):56–63.
15. Dancey JE, Freidlin B. Targeting epidermal growth factor receptor—Are we missing the mark? Lancet 2003;362(9377):62–64.
16. Threadgill DW, Dlugosz AA, Hansen LA, Tennenbaum T, Lichti U, Yee D, LaMantia C, Mourton T, Herrup K, Harris RC, Barnard JA, Yuspa SH, Coffey RJ, Magnuson T. Targeted disruption of mouse EGF receptor: Effect of genetic background on mutant phenotype. Science 1995;269(5221):230–234.
17. Luetteke NC, Phillips HK, Qiu TH, Copeland NG, Earp HS, Jenkins NA, Lee DC. The mouse waved-2 phenotype results from a point mutation in the EGF receptor tyrosine kinase. Genes Dev 1994;8(4):399–413.
18. Weihua Z, Tsan R, Huang WC, Wu Q, Chiu CH, Fidler IJ, Hung MC. Survival of cancer cells is maintained by EGFR independent of its kinase activity. Cancer Cell 2008;13(5):385–393.
19. White E, DiPaola RS. The double-edged sword of autophagy modulation in cancer. Clin Cancer Res 2009;15(17):5308–5316.
20. Yue Z, Jin S, Yang C, Levine AJ, Heintz N. Beclin 1, an autophagy gene essential for early embryonic development, is a haploinsufficient tumor suppressor. Proc Natl Acad Sci USA 2003; 100(25):15077–15082.
21. Koneri K, Goi T, Hirono Y, Katayama K, Yamaguchi A. Beclin 1 gene inhibits tumor growth in colon cancer cell lines. Anticancer Res 2007;27(3B):1453–1457.
22. Song J, Qu Z, Guo X, Zhao Q, Zhao X, Gao L, Sun K, Shen F, Wu M, Wei L. Hypoxia-induced autophagy contributes to the chemoresistance of hepatocellular carcinoma cells. Autophagy 2009;5(8):1131–1144.
23. Cao Q, Yu C, Xue R, Hsueh W, Pan P, Chen Z, Wang S, McNutt M, Gu J. Autophagy induced by suberoylanilide hydroxamic acid in Hela S3 cells involves inhibition of protein kinase B and up-regulation of Beclin 1. Int J Biochem Cell Biol 2008; 40(2):272–283.
24. Yokoyama T, Iwado E, Kondo Y, Aoki H, Hayashi Y, Georgescu MM, Sawaya R, Hess KR, Mills GB, Kawamura H, Hashimoto Y, Urata Y, Fujiwara T, Kondo S. Autophagy-inducing agents augment the antitumor effect of telerase-selve oncolytic adenovirus OBP-405 on glioblastoma cells. Gene Ther 2008; 15(17):1233–1239.
25. Pettaway CA, Pathak S, Greene G, Ramirez E, Wilson MR, Killion JJ, Fidler IJ. Selection of highly metastatic variants of different human prostatic carcinomas using orthotopic implantation in nude mice. Clin Cancer Res 1996;2(9):1627–1636.
26. Mizushima N. Methods for monitoring autophagy using GFP-LC3 transgenic mice. Methods Enzymol 2009;452:13–23.
27. Yousefi S, Perozzo R, Schmid I, Ziemiecki A, Schaffner T, Scapozza L, Brunner T, Simon HU. Calpain-mediated cleavage

of Atg5 switches autophagy to apoptosis. Nat Cell Biol 2006; 8(10):1124–1132.

28. Canil CM, Moore MJ, Winquist E, Baetz T, Pollak M, Chi KN, Berry S, Ernst DS, Douglas L, Brundage M, Fisher B, McKenna A, Seymour L. Randomized phase II study of two doses of gefitinib in hormone-refractory prostate cancer: A trial of the National Cancer Institute of Canada-Clinical Trials Group. J Clin Oncol 2005;23(3):455–460.
29. Curigliano G, De Braud F, Teresa Sandri M, Renne G, Zorzino L, Scardino E, Rocco B, Spitaleri G, De Pas T, Noberasco C, Nole F, Verweij F, Matei V, De Cobelli O. Gefitinib combined with endocrine manipulation in patients with hormone-refractory prostate cancer: Quality of life and surrogate markers of activity. Anticancer Drugs 2007;18(8):949–954.
30. Gravis G, Bladou F, Salem N, Goncalves A, Esterni B, Walz J, Bagattini S, Marcy M, Brunelle S, Viens P. Results from a monocentric phase II trial of erlotinib in patients with metastatic prostate cancer. Ann Oncol 2008;19(9):1624–1628.
31. Small EJ, Fontana J, Tannir N, DiPaola RS, Wilding G, Rubin M, Iacona RB, Kabbinavar FF. A phase II trial of gefitinib in patients with non-metastatic hormone-refractory prostate cancer. BJU Int 2007;100(4):765–769.
32. Marks RA, Zhang S, Montironi R, McCarthy RP, MacLennan GT, Lopez-Beltran A, Jiang Z, Zhou H, Zheng S, Davidson DD, Baldridge LA, Cheng L. Epidermal growth factor receptor (EGFR) expression in prostatic adenocarcinoma after hormonal therapy: A fluorescence in situ hybridization and immunohistochemical analysis. Prostate 2008;68(9):919–923.
33. Sherwood ER, Van Dongen JL, Wood CG, Liao S, Kozlowski JM, Lee C. Epidermal growth factor receptor activation in androgen-independent but not androgen-stimulated growth of human prostatic carcinoma cells. Br J Cancer 1998;77(6):855–861.
34. Traish AM, Morgentaler A. Epidermal growth factor receptor expression escapes androgen regulation in prostate cancer: A potential molecular switch for tumour growth. Br J Cancer 2009;101(12):1949–1956.
35. Goel S, Hidalgo M, Perez-Soler R. EGFR inhibitor-mediated apoptosis in solid tumors. J Exp Ther Oncol 2007;6(4):305–320.
36. Rodeck U, Jost M, Kari C, Shih DT, Lavker RM, Ewert DL, Jensen PJ. EGF-R dependent regulation of keratinocyte survival. J Cell Sci 1997;110(Pt 2):113–121.
37. Harari PM, Huang SM. Combining EGFR inhibitors with radiation or chemotherapy: Will preclinical studies predict clinical results? Int J Radiat Oncol Biol Phys 2004;58(3):976–983.
38. Jost M, Gasparro FP, Jensen PJ, Rodeck U. Keratinocyte apoptosis induced by ultraviolet B radiation and CD95 ligation—Differential protection through epidermal growth factor receptor activation and Bcl-x(L) expression. J Invest Dermatol 2001; 116(6):860–866.
39. Caraglia M, Tagliaferri P, Marra M, Giuberti G, Budillon A, Gennaro ED, Pepe S, Vitale G, Improta S, Tassone P, Venuta S, Bianco AR, Abbruzzese A. EGF activates an inducible survival response via the RAS ▼ Erk-1/2 pathway to counteract interferon-alpha-mediated apoptosis in epidermoid cancer cells. Cell Death Differ 2003;10(2):218–229.
40. Leu CM, Chang C, Hu C. Epidermal growth factor (EGF) suppresses staurosporine-induced apoptosis by inducing mcl-1 via the mitogen-activated protein kinase pathway. Oncogene 2000;19(13):1665–1675.
41. Burdak-Rothkamm S, Rube CE, Nguyen TP, Ludwig D, Feldmann K, Wiegel T, Rube C. Radiosensitivity of tumor cell lines after pretreatment with the EGFR tyrosine kinase inhibitor ZD1839 (Iressa). Strahlenther Onkol 2005;181(3):197–204.
42. Feng FY, Varambally S, Tomlins SA, Chun PY, Lopez CA, Li X, Davis MA, Chinnaiyan AM, Lawrence TS, Nyati MK. Role of epidermal growth factor receptor degradation in gemcitabine-mediated cytotoxicity. Oncogene 2007;26(23): 3431–3439.
43. Morelli MP, Cascone T, Troiani T, De Vita F, Orditura M, Laus G, Eckhardt SG, Pepe S, Tortora G, Ciardiello F. Sequence-dependent antiproliferative effects of cytotoxic drugs and epidermal growth factor receptor inhibitors. Ann Oncol 2005;16(Suppl 4):iv61–68.
44. Abal M, Andreu JM, Barasoain I. Taxanes: Microtubule and centrosome targets, and cell cycle dependent mechanisms of action. Curr Cancer Drug Targets 2003;3(3):193–203.
45. Liu S, Bishop WR, Liu M. Differential effects of cell cycle regulatory protein p21(WAF1/Cip1) on apoptosis and sensitivity to cancer chemotherapy. Drug Resist Updat 2003;6(4):183–195.
46. Higgins LH, Withers HG, Garbens A, Love HD, Magnoni L, Hayward SW, Moyes CD. Hypoxia and the metabolic phenotype of prostate cancer cells. Biochim Biophys Acta 2009;1787(12): 1433–1443.
47. Bajgelman MC, Strauss BE. The DU145 human prostate carcinoma cell line harbors a temperature-sensitive allele of p53. Prostate 2006;66(13):1455–1462.
48. Cheung EC, Vousden KH. The role of p53 in glucose metabolism. Curr Opin Cell Biol 2010;22(2):186–191.

Cancer Research: April 15, 2011; Volume 71, Issue 8, Supplement 1
doi: 10.1158/1538-7445.AM2011-989
Proceedings: AACR 102nd Annual Meeting 2011-- Apr 2-6, 2011; Orlando, FL

Poster Presentations - Altered Metabolic Regulation in Cancer

Abstract 989: Profiling the expression of SGLT1 in prostate cancer

Alicia Blessing[1] and Zhang Weihua[1]

[1]University of Houston, Houston, TX.

Upregulation of the epidermal growth factor receptor (EGFR; HER1; erbB1), a receptor tyrosine kinase, has been linked with increased cell proliferation and decreased apoptosis and thus, with poor prognosis for cancer patients. EGFR has been found to be over-active in most tumors of epithelial origin including: non-small cell lung cancer, breast, head and neck, gastric, colorectal, esophageal, prostate, bladder, renal, pancreatic, and ovarian cancers. EGFR is elevated in prostate cancer cells along disease progression. EGFR tyrosine kinase inhibitors failed to show beneficial effects for prostate cancer patients. Previous studies have found EGFR has kinase independent prosurvival functions. Independent of its kinase activity, EGFR participates in the maintenance of the basal intracellular glucose level of cancer cells by interacting with and stabilizing SGLT1, thus preventing cancer cells from autophagic death. EGFR and SGLT1 do physically interact; however, it was previously unknown whether SGLT1 expression is upregulated along prostate cancer progression. Sodium-dependent glucose co-transporters (SGLTs) are transmemebrane glucose transporter proteins involved in the active transport of glucose. An antibody against human SGLT1 was made and used with immunohistochemistry to show in this preliminary study that SGLT1 is exclusively expressed in the hyperplastic and malignant prostate epithelial cells. SGLT1 was not expressed in the normal epithelial or BPH cells. The results from this study indicate that as the disease progresses, the increased need for glucose within the cells is at least in part being met by the continuous activity of the sodium-dependent glucose co-transporter 1. This potential role of SGLT1 in prostate cancer may provide avenues for new prostate cancer treatments. Future endeavors will focus on designing interfering peptides that ideally will interfere with the SGLT1/EGFR binding, destabilizing SGLT1 in prostate cancer cells, and promoting cell death of prostate cancer.

Citation Format: {Authors}. {Abstract title} [abstract]. In: Proceedings of the 102nd Annual Meeting of the American Association for Cancer Research; 2011 Apr 2-6; Orlando, FL. Philadelphia (PA): AACR; Cancer Res 2011;71(8 Suppl):Abstract nr 989. doi:10.1158/1538-7445.AM2011-989